SELECTIVE ELECTRICAL INTERFACES WITH THE NERVOUS SYSTEM

Wim L. C. Rutten

University of Twente, Biomedical Engineering Department, Faculty of Electrical Engineering & Institute for Biomedical Technology, 7500 AE Enschede, The Netherlands; e-mail: W.L.C.Rutten@el.utwente.nl

■ **Abstract**   To achieve selective electrical interfacing to the neural system it is necessary to approach neuronal elements on a scale of micrometers. This necessitates microtechnology fabrication and introduces the interdisciplinary field of neurotechnology, lying at the juncture of neuroscience with microtechnology. The neuroelectronic interface occurs where the membrane of a cell soma or axon meets a metal microelectrode surface. The seal between these may be narrow or may be leaky. In the latter case the surrounding volume conductor becomes part of the interface. Electrode design for successful interfacing, either for stimulation or recording, requires good understanding of membrane phenomena, natural and evoked action potential generation, volume conduction, and electrode behavior. Penetrating multimicroelectrodes have been produced as one-, two-, and three-dimensional arrays, mainly in silicon, glass, and metal microtechnology. Cuff electrodes circumvent a nerve; their selectivity aims at fascicles more than at nerve fibers. Other types of electrodes are regenerating sieves and cone-ingrowth electrodes. The latter may play a role in brain-computer interfaces. Planar substrate-embedded electrode arrays with cultured neural cells on top are used to study the activity and plasticity of developing neural networks. They also serve as substrates for future so-called cultured probes.

CONTENTS

INTRODUCTION

Definition and Scope of Selective Electrical Interfacing by Neurotechnology

Selective electrical interfacing with the neural system means connecting to neurons, either to their somata or to their axons, on a scale of micrometers.

Neurotechnology operates at the juncture of neuroscience, cellular/tissue engineering, signal processing, and micro-/nanofabrication. Neurotechnology tries to connect the electronic world to the neural world, mainly to the peripheral part of it, via microelectrode arrays. The field is also known as neuroelectronic interfacing or neural engineering (but neural engineering tends to be more broadly construed; see the section below), and it relates to neurotronics or neurobionics. The latter two descriptors reflect the aim of research to restore disturbed muscular or sensory

function and replace natural control. Selective electrical interfacing is involved in both neural stimulation and neural recording.

The specific tissue-metal interface benefits from models and experiments, such as volume-conduction modeling, cell membrane modeling, electrode/electrolyte chemistry, micro-/nanofabrication (silicon, glass, metals), electrophysiology, signal processing, and cellular/tissue engineering. Selective electrical interfacing aims to contact nerve fibers as selectively as possible, requiring devices and fabrication technology in the realm of micrometers. The clinical field of application is neuroprosthesis in rehabilitation medicine, with the goal of restoring sensory or neuromuscular deficits. Another goal is the development of future brain-computer interfaces. Neuroscience research areas that benefit from progress in neurotechnology are the electrophysiology of natural neural networks (brains) and the study of brain slices and cultured neural cell assemblies, including the process of learning in live networks.

Neurotechnology is not the neural analogue of biotechnology: It does not study artificial neural networks. Nor does neurotechnology comprise neuroinformatics or neural dynamics.

Neural Engineering

Neural engineering treats such topics as the neuronal cell, the central and peripheral neural system, computational and experimental models of bioelectric interfaces (stimulation and recording), the neurochemistry of metal-liquid interfaces, the technology of microelectrode array fabrication, cultured neurons and networks, neural prostheses, and artificial learning in ex vivo neuronal networks. It also deals with the successes and problems of such clinically applied prostheses as the pacemaker and the cochlear implant and neuroprostheses of the arm and leg. Finally, it explores computer-brain interfaces, retinal prostheses, and cultured probes (see Table 1).

TABLE 1   Neural engineering topics at various biomedical engineering conferences, 2000–2002

Topic
Neural recording and stimulation (tissue, deep brain, electric, magnetic)
Neural microdevices (arrays, probes)
Neural modeling (ion channel, cellular, system, brain, sensory, motor, forward/inverse)
Neural computation (coding, networks, biomimetic models)
Neural signals (processing, evoked potentials, EEG, brain-computer interface
Neural instrumentation (microsensors, microelectrodes, interfaces)
Neural prostheses (central and peripheral, auditory, visual)
Hybrid and neuromorphic systems (computational, experimental, mixed VLSI)

A Bit of History

Neural and muscular tissue can be activated electrically, either in the natural way or by artificial stimulation, to perform two basic functions: information transport and muscular contraction, respectively.

In 1791, Luigi Galvani (Figure 1) extensively studied muscle contractions evoked by electrical stimulation in his famous experiment on the exposed frog hindlimb nerve-muscle preparation, ascribing the phenomenon to "animal electricity." Galvani (1) concluded that the driving force of the contraction was located inside the preparation. He ignored the fact that two interconnected, different metals evoke a potential difference and that this is the source of stimulation of the nerve, as was recognized later by Volta. Thanks to two centuries of research into membrane electrophysiology (2), we now know that artificial neural excitation requires both membrane activation and an electric stimulus.

Another milestone in neurotechnology was the implantation of an array of 80 electrodes on the visual cortex of a blind woman by Brindley & Lewin in 1968 (3), by means of which phosphenes were elicited. The implant did not much benefit the patient but showed positive results on safety, long-term effectiveness and a leap in the number of channels and amount of conveyed information. It clearly revealed that selective stimulation of small groups of neurons was the goal to strive for, and it showed the accompanying need for high-density microstimulation arrays.

Current research deals with interfaces to cultured neuronal networks and hybrid neural prostheses, among many others. A recent and remarkable discovery is that live, cultured neuronal networks can learn. They can be trained simply and rapidly, using 60-electrode flat-substrate multielectrode arrays (MEAs) (4).

In the years between Galvani's era and our own, electrical stimulation of neural tissue in the human body has been used for many purposes. Pacemakers and cochlear implants have found their way to the patient in everyday clinical practice. Peroneal nerve stimulation to compensate drop foot handicap helps many persons (5). Visual prostheses (6) and brain-computer interfaces (7) are being explored in clinical experimental medicine, as is electrical stimulation to relieve the symptoms of Parkinson's disease (8).

On the recording side of neurotechnology, electrophysiological brain research has traditionally used tungsten or stainless-steel electrodes (single or multiple) to record single- or multi-unit action potentials and to map receptive fields. A newer method uses fluorescent dyes to record activity optically (9). Multielectrode arrays of up to 100 electrodes patterned by photolithography on glass substrates have been

---

Figure 1 (*a*) Luigi Galvani (1737–1798), medical doctor and biomedical engineer. He discovered "animal" electricity, electrical stimulation, and radio waves. (*b*) Galvani's laboratory. The picture shows not only the famous frog preparation (*left*), in which muscle contraction was evoked by stimulation of nerve with a bimetallic arch, but also that radio waves could activate the nerve-muscle preparation. The mechanism producing the radiation stands on the left edge of the table: The rotating disc builds up a static electric charge that eventually discharges into a spark.

(*a*)
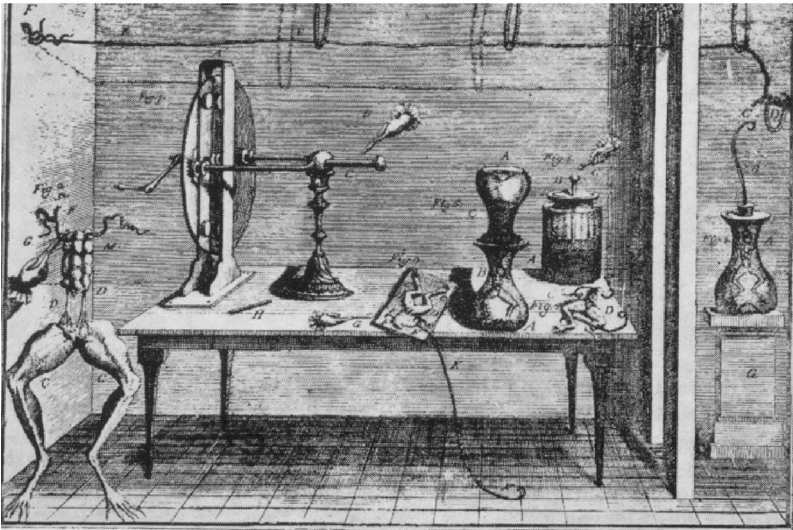
(*b*)

in use since 1972 to record simultaneously from networks, either in retinal tissue ex vivo, in brain slices, or in networks of dissociated neurons.

A selection of neurotechnological principles, applications, and developments is treated or summarized in the following sections.

A Note on Neural Control

Neural interfacing must permit us to exercise neural control. We achieve such control when we know how, where, and when to apply stimuli to affect such functions as bladder control, arm movements, standing, and walking or to enhance or replace the natural coding and processing of sensory stimuli like spoken words or visual images. Interfacing without appropriate control will not lead to clinically useful applications, and vice versa.

THE INTERFACE

Definition of the Interface

As used in neurotechnology, the term "interface" can include all the elements of a system between the central processor of the computer and the nervous tissue—that is, from the data-acquisition interface circuitry; through the wireless electromagnetic link that couples outer world and inner body, the internal wires and electrode tips, and the subsequent tissue volume conductors; to the final target: a whole nerve, a fascicle, an axon, or a soma.

Therefore, the position, shape, and size of an electrode with respect to a neuron or axon determines the precise definition of the interface. For example, if a cultured neural soma covers an electrode completely, and tightly seals it from the extracellular fluid, the interface will consist mainly of the glycocalix. (The glycocalix is the protein matrix-like intermediate substance responsible for adhesion of the cell membrane to the metal or glass substrate. The latter is itself usually coated with a chemical monolayer of an adhesion promoting protein, like laminin or poly-d-lysine.) This layer may be characterized electrically as an ionic fluid, with a certain conductivity and capacitance. If the seal is less tight, currents will leak to the extracellular medium and the interface may be thought of as extended over a larger volume.

Even more components must be considered part of the interface if a cuff electrode contacts a whole nerve, because the conductivity of a fluid layer (between the interior of the cuff and the surface of the nerve) adds to epineural and perineural sheath conductivity, before stimulation currents reach the axonal targets. If the cuff length is short, current leakage into the space outside the cuff must likewise be taken into account.

Definitions of Selectivity

The same variability holds for the definition of "selectivity." Selectivity means that individual target elements may be addressed electrically amidst a population of

identical neighbors. Target elements may be nerves, fascicles, axons, somata, or neuronal processes.

Different levels of selectivity can be distinguished when the aim is to stimulate the motor system or nerves in general. Muscle selectivity implies control (via intramuscular electrodes or cuffs around muscle-specific fascicles) of a specific muscle without activating other muscles. Fascicle selectivity aims at a specific fascicle without activating other fascicles; but fascicle selectivity in general does not guarantee muscle selectivity, as fascicles may innervate multiple muscles.

Size selectivity is possible because thick fibers (with larger inter-node-of-Ranvier spacing) are stimulated at lower current than thinner fibers. (This useful property is hampered by the fact that thin and thick motor fiber have no prescribed position in the fascicle.) Fiber selectivity can only be reached by electrodes, which are small enough and positioned close enough to a fiber, preferably the node of Ranvier. So, tip diameters of a few to about 10 micrometer and positioning not farther than about 20 micrometer from a node are required.

The Nerve Cell Membrane and the Action Potential

Neurons are specialized, nonspherical cells consisting of a cell body (soma), many short dendritic processes, and one longer protrusion called the axon. Axons can be very long (the length of a human arm or leg) or rather short (a pyramidal neuronal cell in the neocortex is about half a millimeter long). Axonal diameter may vary between $<1 \mu$m and $>20 \mu$m. Muscles are controlled by up to a few hundred motor neurons per muscle. The auditory nerve contains 3×10^4 axons and the optic nerve typically 10^6. The brain has 10^{11} neural cells; each cell can have 10,000 connections (see also Table 2).

Neurons communicate information among themselves, muscles, and organs via electrical potentials, called action potentials. Action potentials are short excursions, transient waveforms with a typical duration of 1 ms, from the transmembrane resting potential, which is approximately -60 mV inside versus outside. The polarization is maintained by the mechanism of the so-called sodium (Na^+)-potassium (K^+) pump, which brings about a difference in concentrations of these ions across the membrane.

The membrane is a semipermeable double layer of lipid molecules penetrated by many proteins and containing many pores, or channels (which are filled or lined by protein molecules). A number of them are ion channels to transport ions in and out the cell.

Na^+ and K^+ ion channels play a crucial role in the generation and propagation of action potentials, as they may carry ionic currents through the membrane and perturb the resting potential. The perturbation may be an external short cathodic current pulse, as we will see below in some detail. The channels react to such a pulse by "opening" further, first gradually and linearly but then, beyond a certain depolarization threshold (about 20 mV), in a nonlinear, avalanche-like way. The basic mechanisms of this action-potential generation were discovered by Hodgkin & Huxley (2), Frankenhauser & Huxley (10), and others, who used

TABLE 2 Typical dimensions and numbers in the nervous system

Node of Ranvier length	4 μm
Axon diameter	1−20 μm
Soma diameter	5−20 μm
Nerve fascicle diameter	1 mm
Nerve diameter	several mm
Motor fibers in fascicle	100 s
Auditory fibers	3×10^4
Optical fibers	10^6
Brain neural cells	10^{11}
Connections per brain cell	10^4
Mammalian membrane resting potentials:	
Resting potential of Na$^+$	+55 mV
Resting potential of K$^+$	−102 mV
Resting potential of Cl$^-$	−76 mV

current-clamp and voltage-clamp techniques in squid and frog axons. These researchers also developed analytical models for the action potential, which are still fundamental to more intricate subsequent analysis. Only a brief summary is presented here.

A membrane section can be represented as a parallel RC circuit. Figure 2 illustrates the network representation. The membrane current is the sum of the ionic and capacitive components

$$i_m = i_c + i_{Na} + i_K + i_L,$$

where

$$i_c = C_m(dV_m/dt).$$

The membrane capacitance C_m is constituted by the lipid bilayer. The resistance R, or, more conventionally, the conductance g (with $g = 1/R$), represents parallel ionic channels. The conductances g_{Na} and g_K are variable; they were found experimentally to be functions of the membrane potential V_m and of time t. The leakage conductance g_l is constant (Figure 2). This branch of the circuit also includes the chlorine contribution (so, the chlorine channel has constant conductance).

Under resting conditions the inward sodium current balances the outward potassium current, and the membrane potential is given by

$$V_m = [(g_{Na}/g_K)(E_{Na}) + E_k]/[(g_{Na}/g_K) + 1].$$

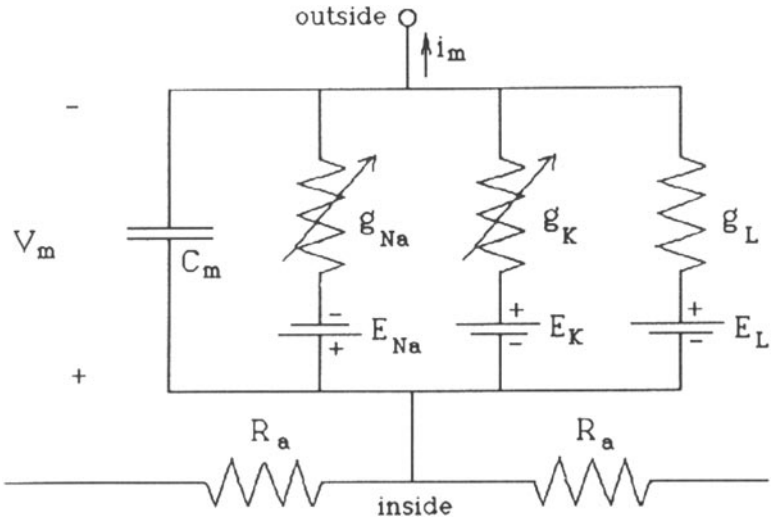At rest, the membrane potential is about equal to the potassium equilibrium

Figure 2 An electrical-circuit-element representation of the neural membrane. Membrane capacitance is about 1 μF/cm^2. E_k and E_{Na} are the driving potentials for the potassium and sodium currents and are given by the Nernst potential. Conductances g_K and g_{Na} are variable while the leakage conductance g_L is constant. V_m is the membrane potential, i_m is the membrane current, R_a is the internal resistance of the axon.

potential E_k ($= -60$ mV); during an action potential V_m approaches E_{Na} ($= +55$ mV). The conductances for the squid axon behave as $g_{Na} = g_{Na,max} \, m^3 h$ and $g_K = g_{K,max} \, n^4$ and have a time dependence, in this case for m, as follows:

$$dm/dt = \alpha_m(1 - m) - \beta_m m,$$

with a possible solution

$$m(t) = m_\infty - (m_\infty - m_0)\exp/(-1/\tau_m),$$

where

$$m_\infty = \alpha_m(\alpha_m + \beta_m) \quad \text{and} \quad \tau_m = 1/(\alpha_m + \beta_m)$$

(with similar expressions for n and h). Parameters α and β depend only on V_m. For example, $\alpha_m = -0.1(V_m + 35)/(\exp[(-V_m - 35)/10] - 1)$. The total set of equations can be solved under space-clamp conditions (i.e., where the membrane behaves uniformly in the direction along the axon, so axial currents are absent):

$$i_m = C_m(dV_m/dt) + g_{Na}(V_m - E_{Na}) + g_K(V_m - E_K) + g_L(V_m - E_L) \quad (1)$$

and yields the intracellular action potential waveform. Rate constant τ_m is much smaller than τ_h and τ_n (so Na channels open earlier in the development of the action potential than K channels).

Artificially Stimulated Action Potentials

While the previous section describes the dynamics of the natural action potential, local extracellular application of a depolarizing (cathodic), monophasic, short ($\sim$100 μs) current pulse (μA range) may excite an action potential, traveling in both directions from the stimulation site. In that case i_m in Equation 1 equals the stimulus current i_s (local microstimulation near a node of Ranvier), and the following equation can be derived and solved for various i_s:

$$dV_m/dt = (1/C_m)[(i_s - g_{Na}(V_m - E_{Na}) - g_K(V_m - E_K) - g_L(V_m - E_L)].$$

Again, this equation is valid under space-clamped conditions, i.e., where no axial currents are present. Repeated, piecewise application of this equation for a partitioned membrane would yield a solvable, coupled set of equations, provided that lateral coupling is introduced. (See the section below on the Nerve Fiber.) An example of transmembrane voltage changes in response to external stimulation is given in Figure 3.

Modeling Electrical Stimulation of Fibers in Peripheral Nerve

Peripheral nerve consists of (up to thousands of) nerve fibers, or axons, with diameters ranging from a few to tens of micrometers. Nerves may contain subbundles, called fascicles, with a typical diameter of 0.5 mm. Motor fibers are wrapped in a myelin sheath that speeds up propagation of the action potential. At regular intervals, λ, the myelin sheath is interrupted over a few micrometers at the nodes of Ranvier. These are the sites where membrane channels exchange ions, keeping the action potential traveling. The ratio of internode distance to fiber diameter is approximately 100:1. A negative-going extracellular current pulse close to a node may trigger the action potential artificially. This is the basis of artificial electrical stimulation (see above).

Modeling is usually done in two stages: nerve fiber excitation and volume conduction.

THE NERVE FIBER   First, the response of a nerve fiber to an electrical field is modeled (11, 12) and modified (13). For this process, the approximate "activating function" may be used, in which a fiber is considered over a length of three nodes only, modeled by two sections of a passive RC network (Figure 4). The nerve becomes active when the second-order difference f (the activating function) of external node potentials V_e of a central node and its two neighbors exceeds a threshold ($\sim$20 mV). As the exact node positions are unknown and f for a given diameter class of fibers only depends on the internode distance λ, activating functions are calculated for each position x, y, z and x, y, z $\pm$ λ in the fascicle, for each electrode. Thus,
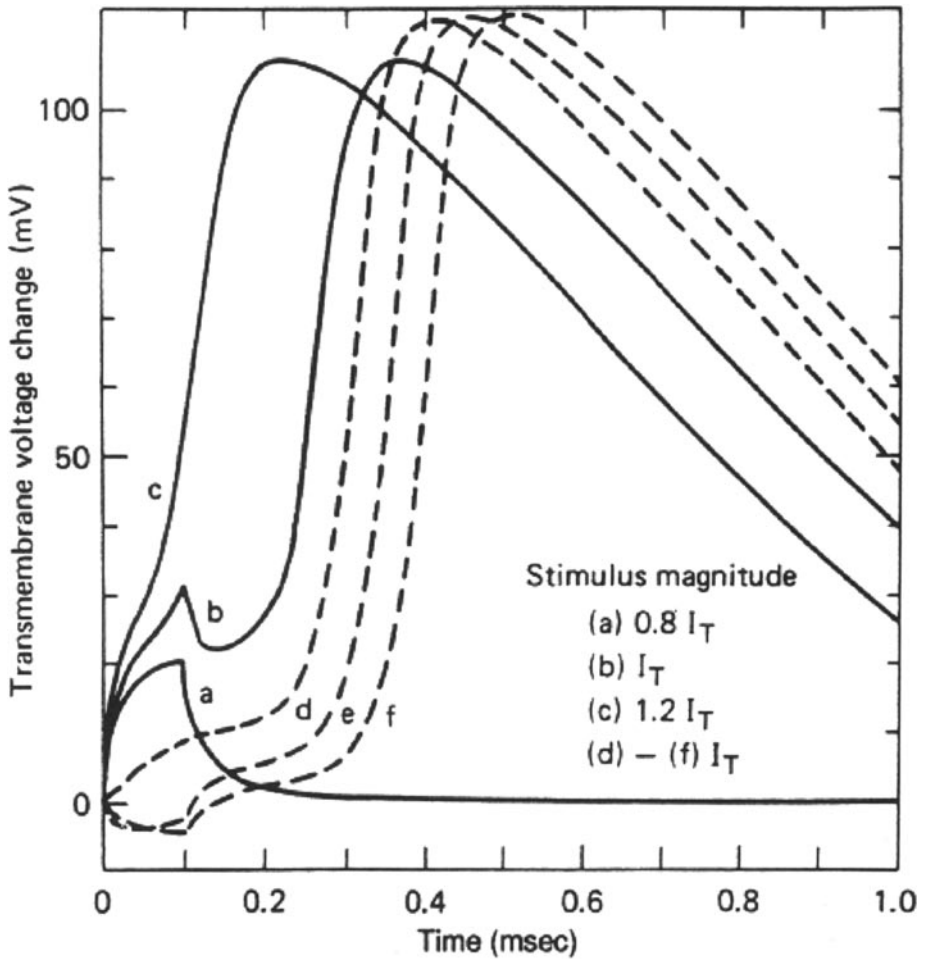
$$\Delta V_n \cong T/R_i C_m f,$$

Figure 3   Action potentials evoked in a myelinated nerve model in response to rectangular monophasic current of $100\ \mu s$ duration, 20-μm-diameter fiber, point electrode 2 mm from central node. The model used by Reilly (120) is a modified version of the McNeal model (11), in which 11 linear nodes are included, adjacent to one nonlinear node. Reilly includes Frankenhauser-Huxley nonlinearities in the 11 adjacent nodes. *Solid lines* show the response at the node nearest the electrode for three levels of stimulus current. *Broken lines* show the propagated response at the next three adjacent nodes for a stimulus at threshold. (Used with permission from Ref. 120, page 112, Figure 4.10).
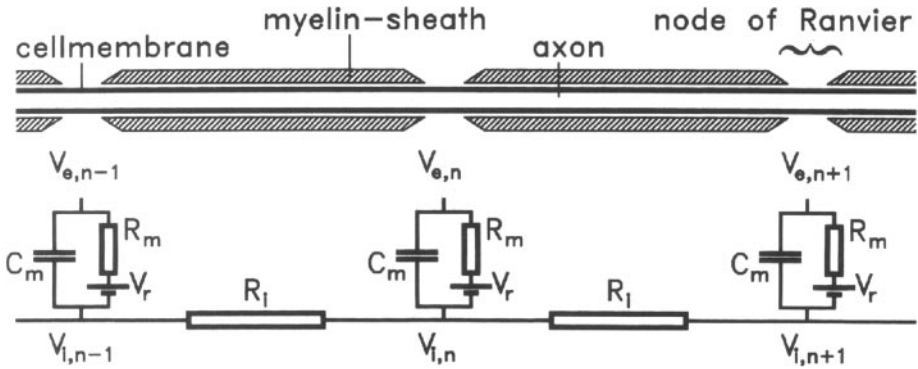
Figure 4   The electric network equivalent of a myelinated fiber. V_r is the membrane rest potential. $V_{e,n}$ is the extracellular potential at node n. $V_{i,n}$ is the intracellular potential at node n. R_i is the intracellular resistance. C_m and R_m are membrane capacitance and resistance.

with

$$f = V_{e,n-1} - 2V_{e,n} + V_{e,n+1} = V_e(x, y, z - \lambda)$$

$$-2V_e(x, y, z) + V_e(x, y, z + \lambda).$$

Meier et al. (13) have shown this to be true for stimulation with a short rectangular current pulse of duration T under the condition that $T < R_i C_m$ and $T < R_m C_m$. A practical value for T is 100 μs.

If an electrode is sufficiently close to a node of Ranvier, compared to λ, the two terms $V_{e,n-1}$ and $V_{e,n+1}$ may be set to zero. This is the "local approach."

Note that the activating function sets the external potential condition but does not take into account ionic currents through the membrane ion channels, which can be modeled by the Hodgkin-Huxley equations and their refined forms. Because of this, the activating-function approach is only valid for short rectangular stimulus-current pulses in the range of 10–100 μs. Also, the well-known relationship at threshold of stimulation between amplitude and duration of the stimulus (the "strength-duration threshold curve") is not contained in the activating function. The effect of pulse duration has been taken into account by Warman et al. (14), Nagarajan & Durand (15), Grill & Mortimer (16), and others. Pulse duration may be a tool to influence spatial selectivity of stimulation.

The activating function above explains the (inverse linear) dependence of stimulus-activation threshold upon fiber diameter for an electrode positioned 1 mm from a nerve fiber (diameter ∼10 um). It takes into account that the ratio of node spacing to fiber diameter is a constant with value of about 100 in a myelinated fiber (11). Note that this is the "inverse recruitment order" property of artificial stimulation. Note, too, that this drawback has no meaning for selective stimulation, which must be local by definition, at approximately no more than tens of micrometers from a node of Ranvier.

The continuous version of, e.g., the second spatial axial derivative of the activating function also explains why a nodic blocking may occur in unmyelinated fibers if a cathodic pulse is elevated to eight times its strength at threshold (12). One may call this a "stimulation window." Again, it is not of much importance when enough electrodes, each close to a different fiber, are available.

THE VOLUME CONDUCTOR   In the second stage of modeling, the potentials $V_{e,n}$ generated by currents from stimulating electrode configurations must be calculated at the node positions of all fibers and represented as equipotential contours or equiactivation function contours (13). Figure 5 shows the volume conductor model of a cylindrical nerve or fascicle. The fascicle is idealized as an electrically homogeneous and infinitely long extending cylinder with a radial conductivity σ_r and a longitudinal conductivity σ_z. The cylinder is surrounded by a layer that represents
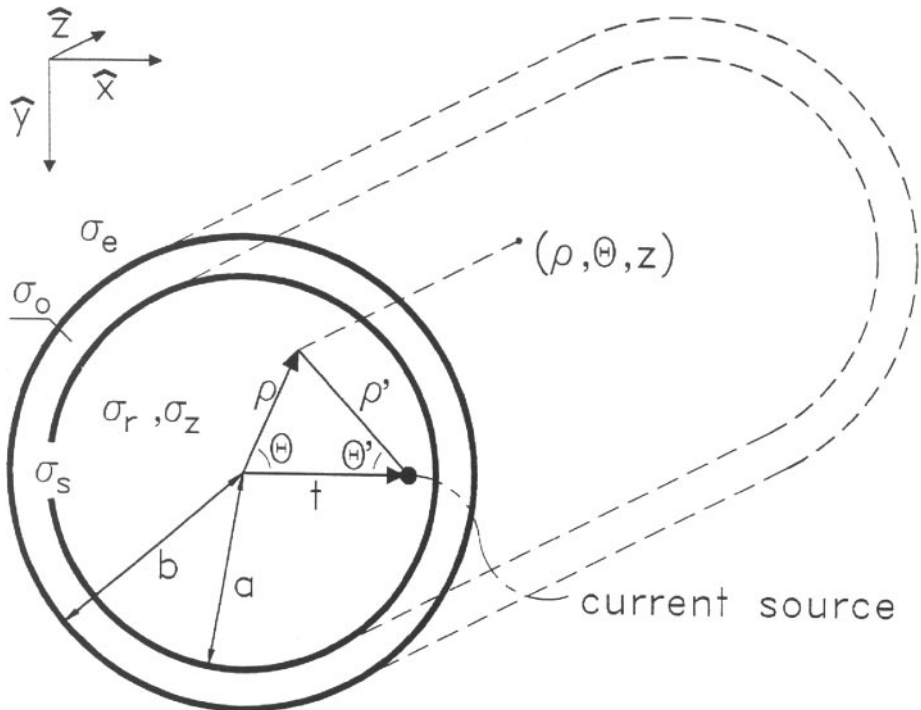
Figure 5   The volume conduction model of the nerve and its surroundings. Longitudinal and radial conductivity inside the fascicle are σ_z and σ_r, respectively. Perineural sheath conductivity σ_s, epineural conductivity σ_o, and extraneural conductivity σ_e are shown. In this model configuration, Poisson's equation is solved analytically. It yields the potential anywhere in the nerve for a stimulation electrode current source at an arbitrary position inside the nerve (13).

the thin perineurium, with a sheath conductivity σ_s. The next layer is the perineurium, with conductivity σ_o. At the outside of the fascicle the medium is infinitely homogeneous and isotropic, with conductivity σ_e. Stimulation electrodes are idealized as point current sources and may be positioned anywhere in the fascicle. Using the cylinder symmetry, an analytical expression for the potentials can be derived. The potential V_e for an electrode at (r, 0, 0) injecting current *I* consists of the sum of a source term V_e^s,

$$V_e^s(x, y, z) = \frac{I}{4\pi \sqrt{\sigma_r \sigma_z} \sqrt{(x-r)^2 + y^2 + z^2 \sigma_r \sigma_z}}, \tag{2}$$

and a boundary term V_e^b, which is an expansion of Bessel functions. Similarly, V_e^s (x, y, z + λ) follows from Equation 2.

Electrode configurations may be monopolar, bipolar, tripolar, etc. Combinations of anodes and cathodes may yield some field-steering capability, although at the expense of higher stimulus currents (13, 17). While the cylindrical idealization of the nerve or fascicle permits the analytical solution of Laplace's equation, as summarized above, the more general case of a nerve volume conductor with many irregular, inhomogeneous, anisotropic fascicular cross sections inside asks for finite-difference modeling of the tissue (18, 19).

Metal Microelectrodes

The metal electrode, with its interface to the electrolytic fluid environment, is an important part of the stimulation system. Metal electrodes in a body-fluid environment are electrochemical transducers; they may exchange electrons with ions (carrier exchange) and/or operate in a capacitive way. The electrode-electrolyte interface is not yet fully understood. Basically there are capacitive mechanisms (charging and discharging of the electrode double layer, no electron transfer) and Faradaic mechanisms (chemical oxidation or reduction, reversible or irreversible). Approximations are made for the Helmholtz layer impedance, the capacitive mechanisms, and Faradaic current. In general, the diffusion and recombination of metal ions in and out of the liquid is a nonlinear charge-transfer process. In practice, charge recovery methods to reach charge balance are necessary for the avoidance of tissue damage by direct currents (20).

The double layer is not simply represented by a lumped capacitor of constant value. In a simple parallel RC representation both R and C depend on frequency in the range up to 10 kHz. They decrease with increasing frequency and may vary with $f^{-\alpha}$, with α depending on the metal, the presence of absorbed compounds on the metal, the rate constants of chemical reactions, and many other circumstances. For example, in physiological saline, α is 0.5 and the phase angle between real and imaginary parts of the impedance is $45°$.

Around 1973, selection of a microelectrode meant the choice between a glass micropipette (for intracellular recording) or a metal microelectrode (for extracellular purposes). Metals were platinum, tungsten, stainless steel, or indium. Later, Pt/W and Pt/Ir electrodes (21), with improved impedance characteristics,

became available. Specifically, they behave better at low frequencies, compared, for example, to the average $f^{-0.75}$ frequency dependence for Pt (22).

The smaller the area of a microelectrode, the higher its impedance. Enlarging the surface in the form of a porous coating (Platinum-black) or columnar structure (titanium nitride) can compensate for this phenomenon. Compensation is not needed so much for stimulation purposes, but because noise accompanies impedance (for thermal noise of resistive origin, $V_{rms} = \sqrt{4kTR\Delta f}$; for example, 1 MOhm in a bandwidth of 10 kHz yields 12.8 μV-rms), compensation is advisable when recording action potentials. As an example, Figure 6 shows the surface of a TiN-coated electrode. Such structuring may reduce impedance from a few MOhms to several hundreds of kOhms.

The Neuron-Electrode Interface and Stimulation of Neuronal Cell Bodies

The neuron-electrode interface is electrically characterized by three components: the neuron, the microelectrode, and the medium in between. As selective stimulation requires close contact with the cell, the medium will in general have the form of a neuron-electrode gap. If the contact specifically concerns the contact of a (patch) glass pipette electrode on the soma of a brain cell, or a dissociated neuronal cell (in a culture dish, for example; see below) adhered to a microelectrode array substrate, the gap may be very narrow, between 30 and 300 nm. The cell may even "seal" the electrode (or electrode well) completely. What happens there deserves further consideration. Depending on the sealing quality or the position of electrode near the soma, axon, or axon hillock, the stimulation site and stimulation process may differ.

In his 1975 review, Ranck (23) concluded that "Stimulation of a neuron near its cell body is not well understood, but in many cases the axon is probably stimulated."

Figure 7 shows the current paths for a sealed-cell-body configuration and its modeling circuit elements.

Recently, a study into the neuron-electrode interface revealed the existence of a stimulation window (24) and elucidated the fundamental understanding of cell-body activation. That a cell exhibits a stimulation window means that it is activated at a certain cathodic threshold [−30 nA in Figure 8] but will ultimately stop firing upon increase of the current. Here the window is different from that of an axon. In this case, the balance of inward and outward ionic membrane currents is disturbed in such a way that ultimately the upper membrane cannot be depolarized enough to initiate an action potential during the stimulus pulse.

Selectivity of Stimulation and the Efficiency of a Stimulation Device

At low current, an electrode can stimulate one fiber if its position is closer to that fiber than to other fibers. Increase of current will expand the stimulation volume—that is, will include more and more fibers. The ultimate selectivity will be reached
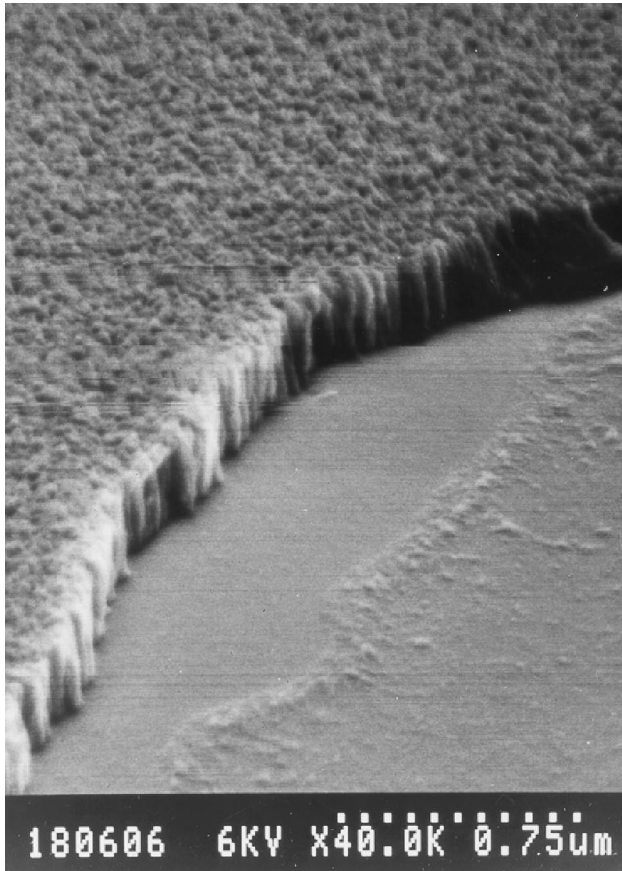
Figure 6   Scanning electron microscope photo of electrode Au surface with deposited TiN columnar structure to increase active surface and thereby lower the electrode impedance (to about 100 kOhm at 1000 Hz, for a 10-μm-diameter electrode). TiN material is deposited by reactive sputtering of titanium in an Ar/N$_2$ plasma. With the correct process parameters, the layer develops a columnar, porous structure. The originally yellow TiN turns black, owing to the fact that no light is reflected (as in platinum black). The TiN layer can be applied to all electrodes at the same time and is mechanically very robust.

if each fiber had its "own electrode." Such a situation would require both enough electrodes and a blueprint of nerve fibers such that electrodes could be positioned close to the nodes of Ranvier. In practice, no blueprint is available and microfabrication has technological limits. Because we must use a limited number of electrodes placed optimally (in a statistical sense), we must consider and test the degree to which stimulation can be selective—that is, the extent to which each electrode
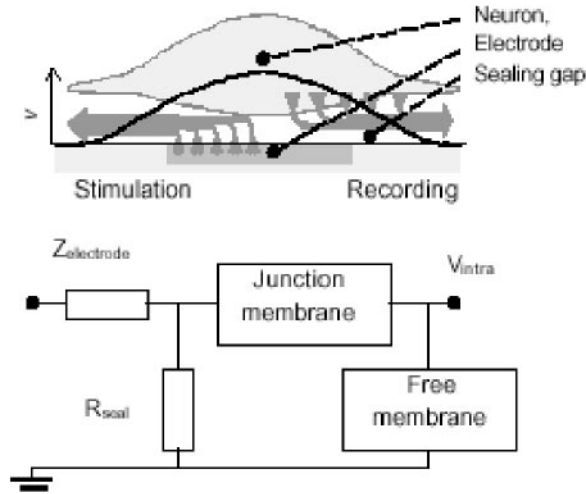
Figure 7 (*upper panel*) Mediation of the neuron-electrode interface in extracellular stimulation and recording. Owing to current densities, arising from the neuronal membrane or the electrode, a potential distribution exists in the sealing gap that modifies the membrane potential (stimulation) or can be probed by the electrode (recording). (*lower panel*) Electrical equivalent lumped circuit of the kind commonly used as a model of the neuron-electrode contact (from Ref. 24, courtesy J. Buitenweg).

controls as few fibers as possible at low current, before potential fields start to overlap with those of other electrodes. Greater overlap means lower selectivity.

From another point of view, one might define the efficiency of a multielectrode device as the number of distinct fibers that can be contacted divided by the total number of electrodes. Greater overlap means reduced efficiency. Fiber selectivity has been addressed by Smit (25) and by Rutten et al. (26) as well as by others. It was concluded, on statistical grounds and by overlap experiments, that an electrode separation of 128 μm was optimal for a rat peroneal nerve fascicle with 350 alpha motor fibers.

Force recruitment experiments in a rat motor nerve using a 2-dimensional (2-D) 24-electrode array with an electrode separation of 120 μm (27, 28) found that 10 distinct threshold forces could be evoked (the efficiency of the device is $10/24 = 42\%$) (see Table 3 and Figure 9). Under less-strict requirements for selectivity, i.e., assuming that distant, nonneighboring electrodes would probably not activate the same motor neurons, the efficiency went up to 81%. Here, efficiency was defined as the ratio between the number of measured distinct force thresholds and the number of electrodes.

Selectivity can also be enhanced by multipolar (e.g., tripolar) stimulation. In a nerve fascicle, a linear anode-cathode-anode combination, positioned with its long axis across the fascicle, will narrow the excitation region considerably (13) (see

TABLE 3   Efficiency of stimulation in rat peroneal nerve (28)

Experiment	E	E′	N_{el}
a	0.80	1	5
b	0.40	0.80	5
c	0.60	0.80	5
d	0.42	0.79	24
e	0.50	0.88	8
f	0.47	0.71	17
g	0.46	0.83	24
h	0.21	0.64	14
Average	0.48	0.81	

Summary of efficiencies E and E′ in eight experiments with the 24-fold 2-D electrode in rat peroneal nerve (Figure 13). Efficiency E is defined as the fraction of the number of electrodes that produce distinct force levels at threshold, implying that these electrodes control a separate muscle unit. If more than one electrode has the same threshold force level, only one counts, as it is assumed that this electrode contacts the same axon going to the same muscle unit. This multiple control is likely for neighbor electrodes but less likely for electrodes that lie farther apart in the array. They will probably control another muscle unit, with an identical force. When these latter electrodes are allowed to be counted, the greater efficiency E′ results. N_{el} is the number of electrodes used in an array. From Ref. (28).

Figure 10). In a cuff electrode, a tripole oriented in the longitudinal direction may theoretically generate unidirectional action potentials in small nerve fibers while blocking the larger fibers (29).

Peripheral Nerve Fiber Recording: Modeling and Selectivity

The forward control of muscle by artificial stimulation might gain importance when this control is supplemented by selective feedback information from nerve fibers attached to sensors such as muscle spindles, tendon organs, and cutaneous sensors. This asks for insight into selective recording with multielectrodes. The same type of calculation as previously made for selective stimulation of nerve fibers in rat peroneal nerve (isotropic conductor, local approach) (26) could be applied, by reciprocity, to the case where the device is used to sense natural activity from afferent fibers. These calculations would lead to a (statistically optimal) electrode interdistance of 143 μm for the case where there are 250 type I afferent fibers in rat peroneal nerve. But, while an action potential can be triggered by activation of only one node of Ranvier (stimulation), propagation of an action potential inevitably involves about 20 active nodes (recording). Therefore, in such calculations one cannot replace the electrode (stimulation) by one node of Ranvier (recording) and make a reciprocal model. In other words, the problem is not symmetrical; forward and inverse calculations are different.
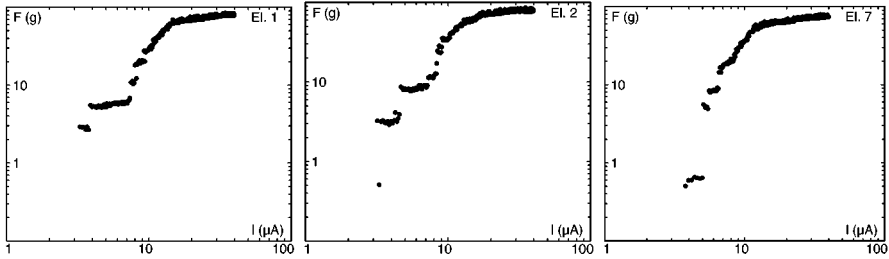
Figure 9   Motor unit recruitment curves, stimulated by the inserted 24-fold microelectrode array of Figure 13, showing twitch force of EDL muscle (vertical scale in newtons) versus stimulus current amplitude (in μA of 0.1-ms-wide rectangular pulse). Three electrodes are shown. Each curve corresponds to a single electrode and is the result of applying a series of single stimuli with amplitudes increasing from 1 μA to 40 μA in steps of 0.1 μA. The noise threshold of the force transducer employed lies at 4.9 mN. Data below this are not shown. Plateaus and steps in the beginning of the curve mean selective stimulation: The electrode's stimulus field expands with increasing current and "meets" motor fibers one by one. For ideal selectivity, the threshold force is unique per electrode, belonging to a specific motor unit at that specific electrode (from Ref. 28).
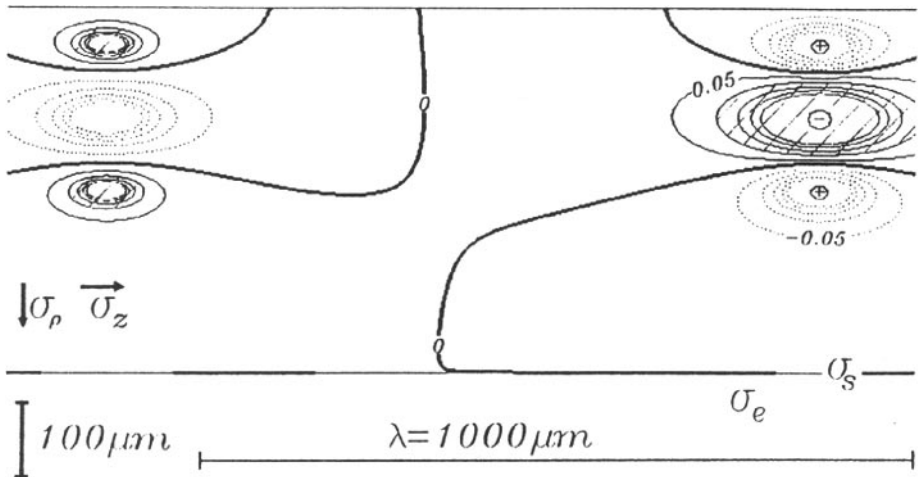

Figure 10   Tripolar-stimulation activation-function isocontours, drawn in a longitudinal cross-sectional plane through the nerve. Isovalues are given in volts. In the hatched areas the value of this function is higher than 0.1 V, which corresponds to a membrane depolarization of about 20 mV, i.e., activation threshold. The calculations are for fibers with an internodal length λ of 1 mm. The hatched area means that fibers that run longitudinally through this area will be stimulated. In the tripolar area at the right, the stimulation is cathodal (*central ellipses*, *solid lines*). In the two "satellite" regions in the left part, stimulation is anodal (*solid ellipses*). The nerve bundle is modeled homogeneously and is immersed in a good conducting medium. Conductivity parameters: $\sigma\rho = 0.1\ \Omega^{-1}\ m^{-1}$, $\sigma_z = 0.5\ \Omega^{-1}\ m^{-1}$, $\sigma_s = \propto \Omega^{-1}\ m^{-1}$, $\sigma_e = \propto \Omega^{-1}\ m^{-1}$, stimulus currents $I_{cath} = 20\ \mu$A, $I_{an} = 10\ \mu$A (from Ref. 13).

Another difference between stimulation and recording is that nerve fibers will almost always fire as ensembles. When two (not overlapping in time) action potentials (or action potential trains) are sensed by one electrode, the trains can be detected separately when the selectivity ratio S of their amplitudes V_1 and V_2 exceeds a certain threshold, i.e., when $S > S_{th}$, for example, $S > 1.1$, or $S > 2$ (compare this to signal to noise ratio; 1.1 means barely visible, 2 is better). Quantitative insight in this selectivity ratio S as a function of spatial and conductivity parameters may be obtained by the combined use of an electrode "lead field" model (using the volume conduction model as outlined above) and a probability model for the positions of active fibers (30). Figure 11 shows a dramatic decrease in the ability to discriminate two trains when the nerve is insulated from its surrounding tissue (i.e., for zero extraneural conductivity), illustrating the importance of a natural "wet" surrounding of the nerve.
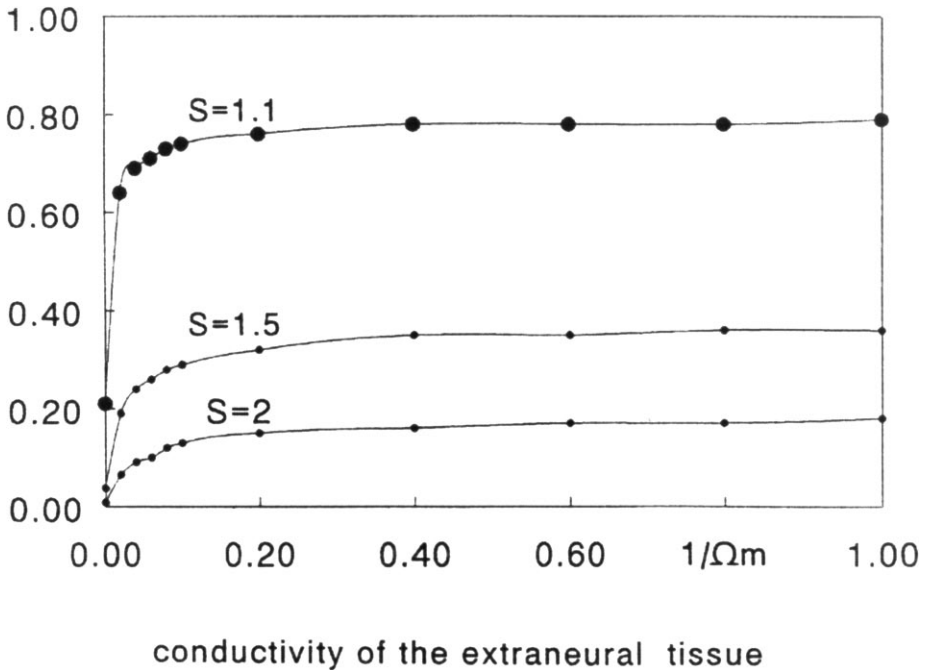

conductivity of the extraneural tissue

Figure 11   The probability P (*vertical axis*) that the measured action potentials from the two fibers nearest a central monopolar electrode have an amplitude ratio $S > S_{th}$. Results are shown for three thresholds (1.1, 1.5, and 2) as a function of the conductivity of the extraneural tissue. The nerve has 40 active fibers (with 20 nodes each) (from Ref. 30). Note that in a nerve surrounded by an isolating medium (like air) fibers cannot be discriminated by their amplitude ratio (left part of the curves all tend to zero).

PENETRATING ELECTRODES

Microfabricated Linear, 2-D, and 3-D Multielectrodes

"Linear multielectrodes" refers to a one-dimensional array of electrode sites mounted in/on a needle or incorporated in a glass or silicon tip-shaped carrier. The needle is a hollow metal shaft in which a side-window perforation houses the tips of a number of leads threaded through the shaft. More-recent technology (31) allows the lithographic patterning and deposition of thin-film metal leads and electrode sites onto glass, silicon, or polyimid carriers (Figure 12). A 2-D array consists of electrodes, with the tips in the same plane, configured either as a bundle of wires (Figure 13) or as galvanically grown needles (Figure 17). When the array is slanted (Utah Slanted Electrode Array, Figure 14) or needles have otherwise variable lengths (UT-array, Figure 15) such that the tips are no longer in the same plane, these structures are called 3-D because such penetrating structures offer the best spatial selectivity [details follow in the next two paragraphs and a separate section is devoted to multielectrode arrays (MEAs)].

Silicon and Silicon-Glass Arrays

Silicon-based microprobe fabrication has been an outstanding activity of the Center for Integrated Sensors and Circuits at the University of Michigan. It has led to a large number of single-shaft, multi-shaft, and 3-D stacked microelectrode arrays, a number of these being supplied with onboard microelectronics (32–41). Design studies (42), strength characterization (43), and development of interconnection technology (44–48) have supported fabrication. Groups in Utah and Twente fabricated "brush" or "needle-bed" 2-D/3-D multielectrodes with about 100 electrodes in silicon or silicon-glass technology, for cortical and nerve applications. As anisotropic silicon etching cannot (yet) achieve the aspect ratios needed for long, slim needles (a needle 20 μm in diameter and 500 μm long has an aspect ratio of 25), the first step in obtaining a brush structure from a solid piece of silicon is a sawing procedure (30, 49, 50). Silicon-glass technology has the advantage of high aspect ratios, sufficient length of needles, and different lengths of needles in the same device. Its disadvantages are the 3-D nature of many of the process steps, the large number of steps, and the difficulty of their integration. Nevertheless, two prototypes of 128-electrode (addressable) devices mounted on a processing chip (CMOS gate-array mixed-mode technology) have been realized (Figure 15) (30, 51, 52). The Michigan group's (39, 53; Figure 16) 3-D cortical multielectrode array, using microassemblies of 2-D planar probes, is a good example of a hybrid fabrication solution: stacking of multishaft/multisite flat devices.

Silicon-LIGA Arrays

An alternative, batch-oriented, and larger-scale way to fabricate multielectrode needle-shaped devices is to combine silicon technology with the LIG
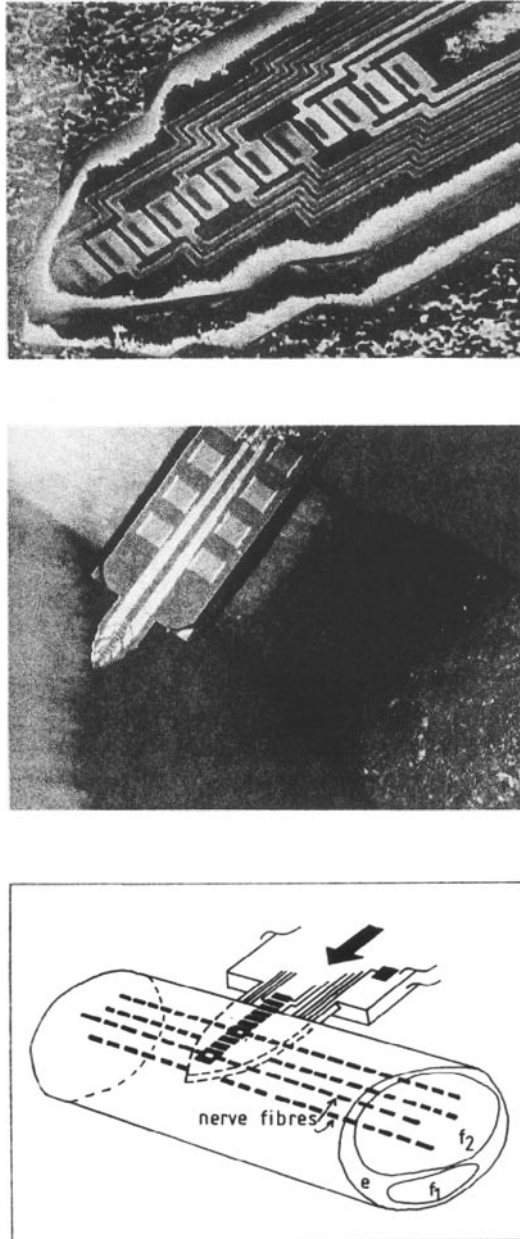
Figure 12   (*top*) 1-D silicon tip-shaped array with 12 platinum electrode sites 50 ×
50 μm at a distance of 50 μm from each other. Insulation layer is Si_3N_4, tip thickness
is 60 μm. (*middle*) The device against the tip of a match. (*bottom*) Insertion of the tip
device into fascicle f2 of a typical peroneal nerve trunk of a rat (diameter 0.5 mm)
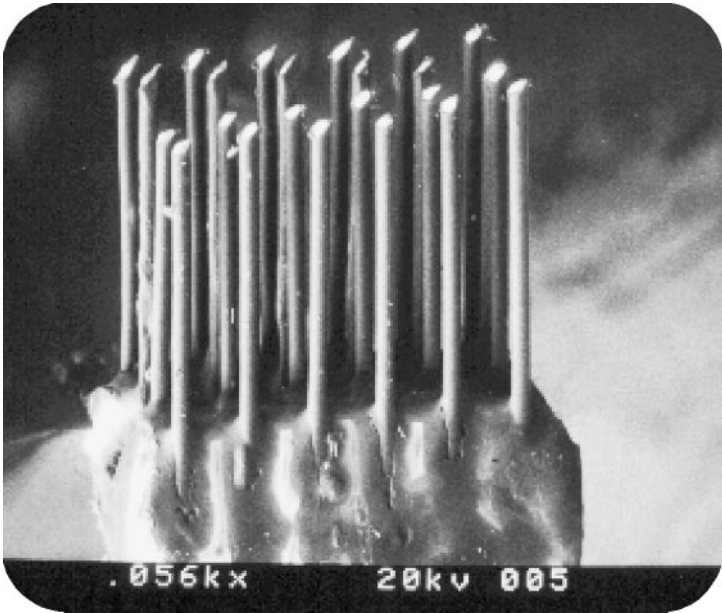(from Ref. 26).

Figure 13 Micrograph of 24-fold 2-D wire electrode array; electrode spacing is 120 μm (from Ref. 28).

(Lithographie, Galvano Abformung) technique (53). In the silicon-LIGA process, nickel needles are grown from a combined seed/interconnection layer through narrow channels in 200 μm PMMA (polymethylmethacrylate). After removal of PMMA and etching of the seed layer, the electrode needles, which stand completely electrically separated, are connected individually to the leads in the interconnection layer. Using this technique at the Institut für Microtechnik in Mainz, Germany, Bielen fabricated a 2-D multielectrode of 4 × 32-needle electrodes, with square as well as round columns or needles. They have a thickness as low as 15 μm and a height of 150 μm (54), as illustrated in Figure 17. Ultimate heights attained were 400 μm. Silicon-LIGA technology reduces the number of steps but has the disadvantage of requiring synchrotron radiation facilities. Even at its present needle-length limit (400 μm), the LIGA + electroplating process facilitates useful neuroprosthetic and cortical applications.

Other Interfaces

An interesting, nonsilicon approach to making contact with fibers intrafascicularly is the use of tethered Pt microwires (25 μm diameter) developed by Horch and colleagues (55–61).
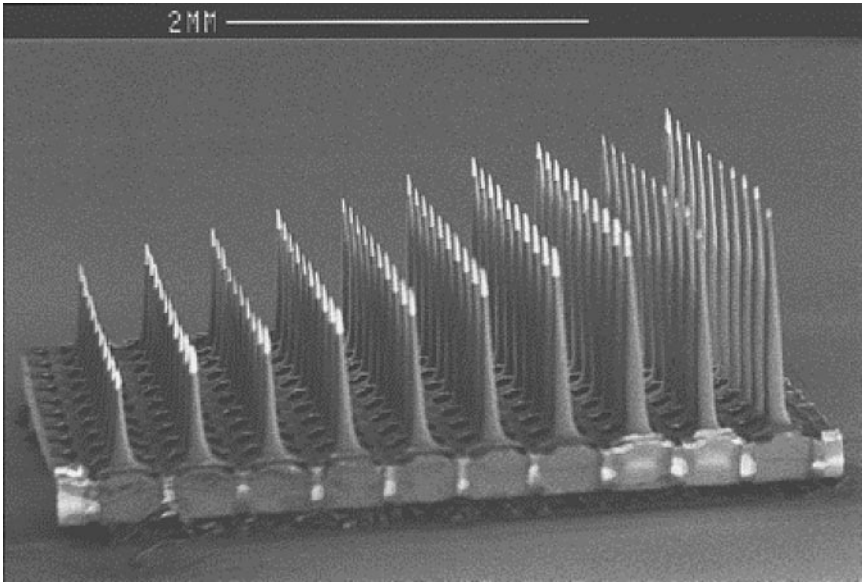
Figure 14   The Utah Slanted Electrode Array. The needles are conductive owing to the use of doped silicon and are electrically insulated with silicon nitride. Only the platinum-plated tips are exposed, with an area of about 0.005 mm^2. The electrodes are regularly spaced on 400 μm centers. The electrode lengths range from 0.5 to 1.5 mm, with 0.1 mm difference in length between rows of neighboring electrodes. Each electrode is approximately 80 μm wide at its base and tapers to a sharpened tip (from Ref. 114).

CUFF ELECTRODES

Cuff electrodes are placed on the inside of a tubular cuff wrapped around a nerve (split cylinder or spiral cuff). They have been in use since 1974/1975 (62, 63). The number of electrodes in a cuff may vary, but it is usually below ten. Cuff electrodes may offer a degree of fascicular sensitivity. The electrodes may be micro-size electrodes. But, as selectivity is fascicle selectivity, electrode sizes may also be in the (sub)-millimeter range. Cuffs may be designed for blocking neural transmission [e.g., collision block (64)], they may recruit fibers in a more natural order (65), or they may be chosen because the nerve of interest is too delicate (lies too deep or has fibers too thin) for the use of penetrating electrodes (6). For recording, the insulating cuff permits higher amplitudes because the current is shielded against leaking away, but at the same time recording selectivity decreases (66). Tripolar arrangements suppress noise. A longitudinal tripole may theoretically generate unidirectional action potentials in small nerve fibers while blocking the larger fibers (collision block) (29).
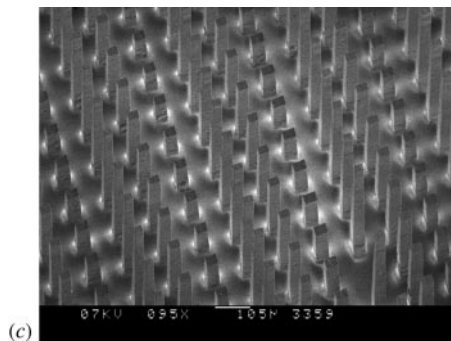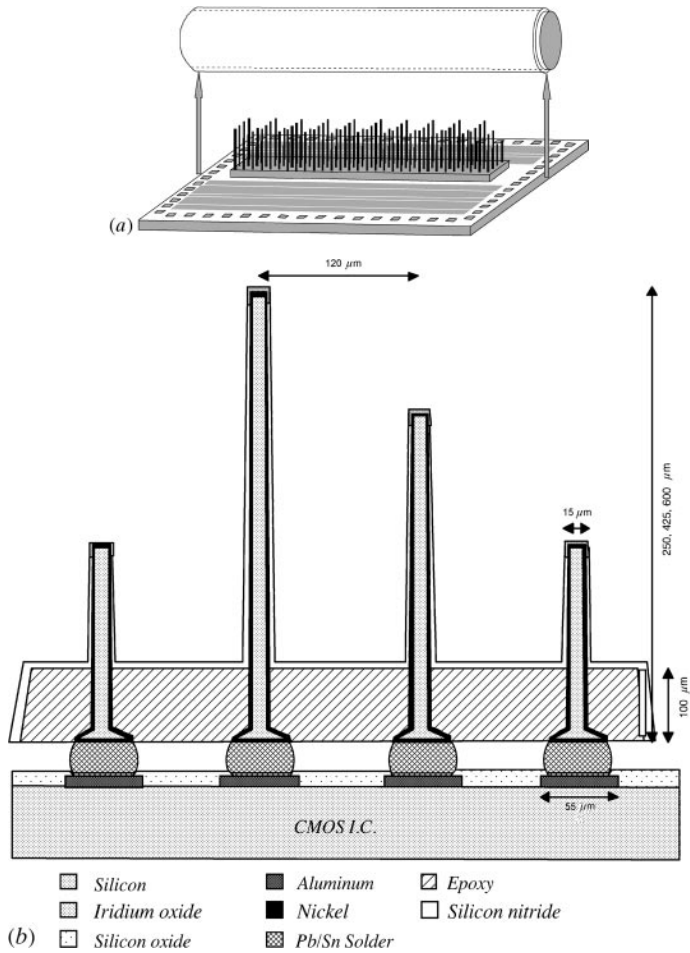
120 μm

250, 425, 600 μm

15 μm

100 μm

55 μm

CMOS I.C.

☐ Silicon	■ Aluminum	▨ Epoxy
☐ Iridium oxide	■ Nickel	☐ Silicon nitride
☐ Silicon oxide	▨ Pb/Sn Solder	

(b)

07KU   095X   105M 3359

(c)

Figure 15 (*a*) Scheme of the University of Twente 128-electrode 3-D glass-silicon array (UT-128 array), mounted on a CMOS, mixed mode processing chip with dimensions 4×4 mm. Needle length is 600, 425, or 250 μm; width at tip is 15 μm; and needle spacing is 120 μm. (*b*) Details of the dimensions and materials used for the UT-128 array. (*c*) A "sea" of sawn and etched silicon needles of three different lengths, embedded in a glass matrix.

(a)

(b)
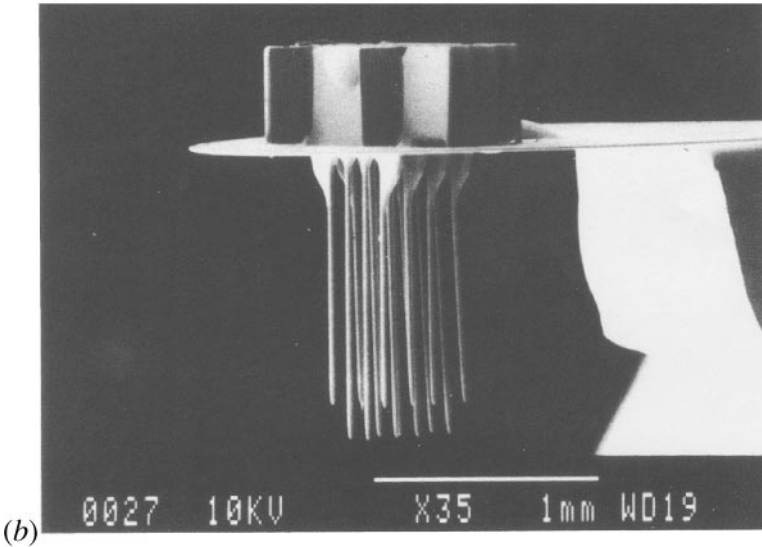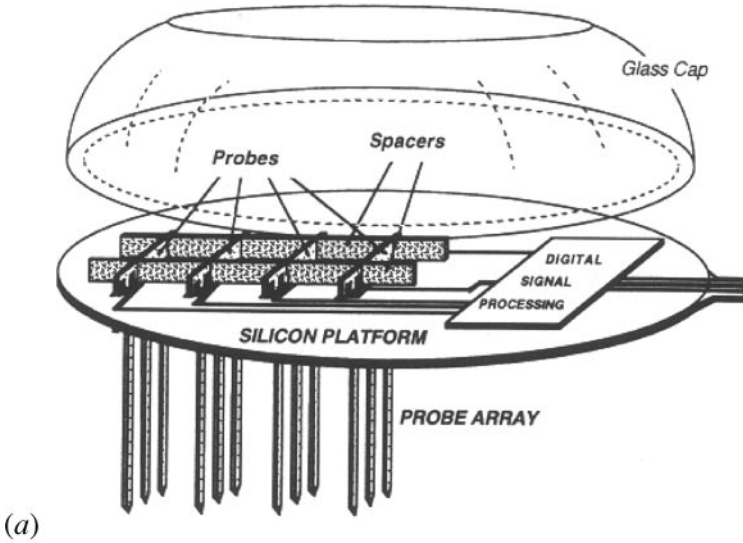
Figure 16 (*a*) Overall diagram of a surface-mounted 3-D recording array. Several multishank 2-D probes are inserted through the platform and held in place with micromachined spacer bars (from Ref. 39). (*b*) Scanning electron microscope (SEM) photographs of a 3-D, 4×4-shank microelectrode array. The shanks on the same probe are spaced on 150 μm centers and are 40 μm wide. The probes are 120 μm apart in the platform (from Ref. 39).
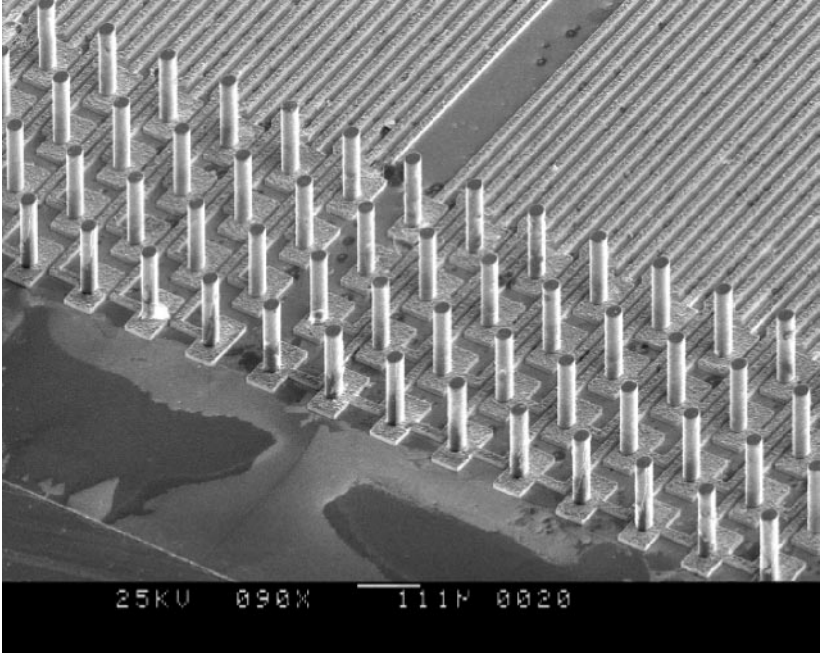
Figure 17   SEM photograph of array with 150-μm-tall, 20-μm-diameter nickel needles, realized with aligned X-ray LIGA on silicon substrate with 8-μm Cu interconnection wiring. Interdistance between columns is 120 μm (from Ref. 54).

The affects of long-term application and the degree of damage caused by neural electrodes is best documented for cuffs. Cuffs are usually designed to be wider (50%) than nerve diameter to avoid compression and subsequent neural damage. They may be self-sizing. Also, leads must be very flexible, and nerves should have enough slack to avoid damage from mechanical movements of cuff and leads, e.g., edema, connective tissue formation, degradation in performance, or, ultimately, death of the nerve. Although longer cuffs give more signal amplification in recording, from a mechanical point of view, shorter cuffs are preferable.

REGENERATION SIEVES AND
CONE-INGROWTH ELECTRODES

Above we considered insertion of multielectrodes into peripheral nerve. As noted, if a microelectrode is not exclusive to one target fiber (the overlap problem), its efficiency is reduced.

Three alternative ways to interface electrodes to neurons are the sieve devices, filled-cone electrodes, and planar multielectrode arrays. The sieve lets cut nerve

fibers regenerate through holes in a transverse 2-D array. A "mixed" type of electrode is the cone electrode filled with a neurotrophic substance–like nerve growth factor (NGF). The third interface method involves culturing nerve cells on patterned planar multielectrode substrates. (The latter approach receives attention in the section below on Planar Substrate Embedded Electrode Arrays.) Among other uses, these cultured cells and their networks provide an excellent tool for the understanding of the neuron-electrode interface. All of these electrode types involve the growth of nerve fibers or neurites. If successful, these devices provide close contact to specific nerve fibers, reducing the overlap problem and increasing electrode efficiency.

Regeneration Sieve Microelectrode Arrays

A regenerative method of interfacing nerves to electrodes is the use of a 2-D (planar) sieve between the two cut ends of a nerve (Figure 18). The silicon sieve permits nerve fibers to regenerate through metallized hole (or slit) electrodes in the sieve (67–71). The main advantage of this method is that microfabrication of flat devices is easier than that of 3-D devices. Another advantage is that, once the nerve has been regenerated, the device is fixed firmly to it. However, since the flats are typically only 10-μm thick, there is a limited chance that nodes of Ranvier will be close to an electrode (typical internode spacing of a 10-μm fiber is 1 mm), thereby limiting the selectivity of stimulation/recording at the fiber level. Crosstalk between electrodes was studied by Wallman et al. (72), who confirmed this handicap. Another problem is that nerve fibers tend to grow through holes not as single fibers but as a group (a process called fasciculation) (73), thereby reducing the possibility of selective stimulation. Zhao et al. (70) reported that after 4–16 weeks of regeneration through 100-μm hole diameters, nerves recovered more or less their normal anatomy, but the force in the corresponding muscle declined by 40%. Smaller holes yielded morphological and functional failures. Guidance of neurites through sieves by Schwann cells provides a means of circumventing inhibitory scar formation (74). While most studies use sciatic nerve for regeneration through a sieve, Heiduschka et al. (75) demonstrated that the optic nerve also is a good candidate.

Cone-Ingrowth Electrodes and Brain-Computer Interfaces

In 1989, Kennedy (76) reported on the cone electrode implanted in rat cortex: a long-term electrode that recorded from neurites grown onto its recording surface. The electrode was a gold wire fixed inside a hollow glass cone (1.5 mm long with a tip-opening diameter of 100–200 μm) filled with a piece of sciatic nerve. Stable single-unit and multi-unit neural activity was recorded for months. When nerve growth factor (NGF) replaced the piece of sciatic nerve, no ingrowth was observed, perhaps owing to leakage of NGF out of the cone. In a later paper (77), the application was confirmed for monkey and for neurotrophic medium fill, with histologic examination suggesting again that ingrowth of cortical neurites
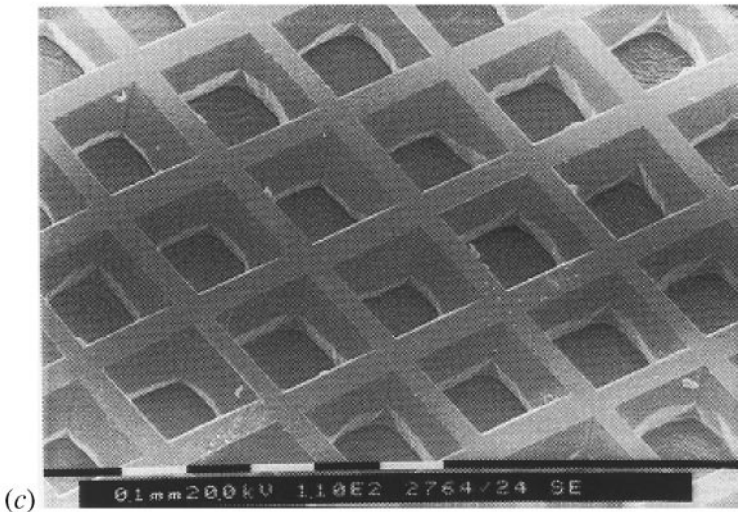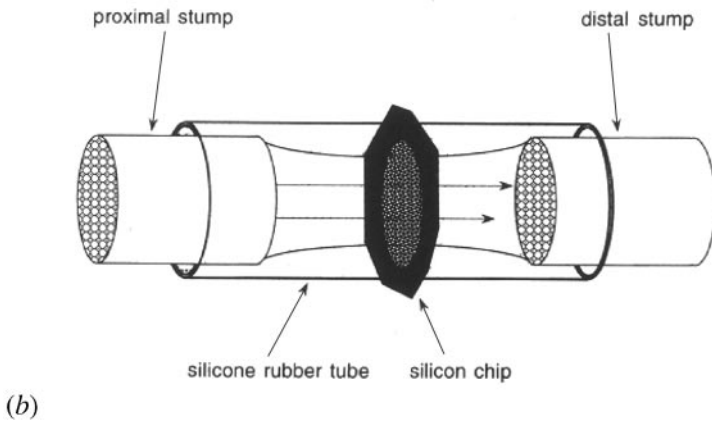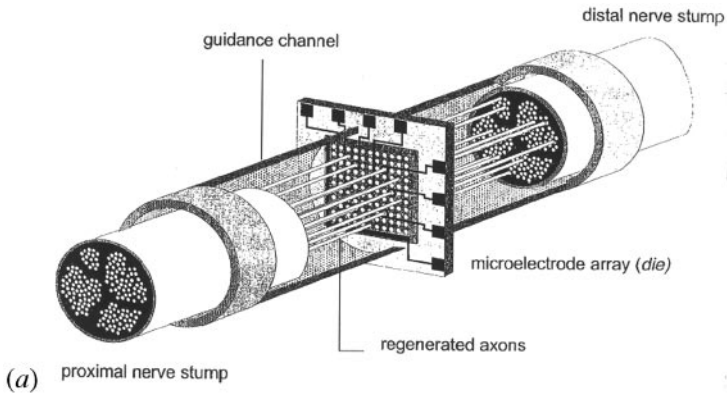
(a)

(b)
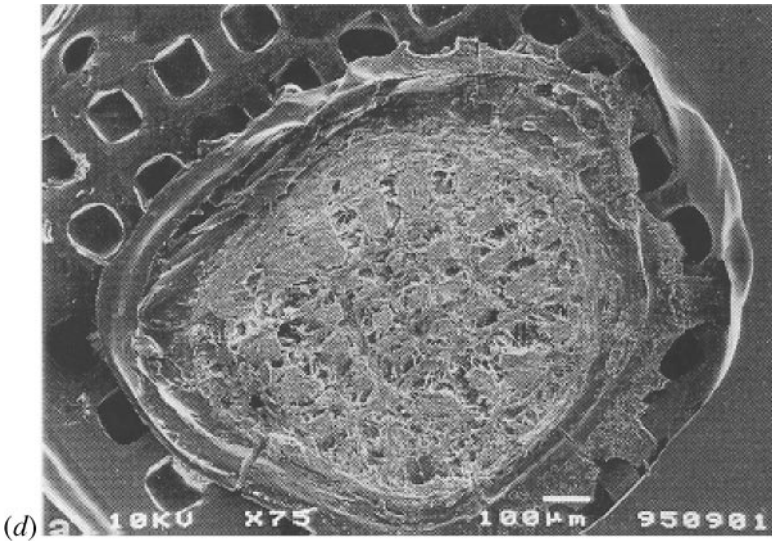

(c)

Figure 18 (*Continued*)

Figure 18   (*a*) Schematic representation of an intelligent neural interface (sieve array) implanted into an intersected nerve (from Ref. 71, Figure 1). (*b*) Schematic drawing of the silicone chamber model with the inserted silicon chip bridging a 4-mm gap between the proximal and distal stumps of a transected rat sciatic nerve. (from Ref. 70, Figure 3). (*c*) Detail of the sieve. SEM photograph of a fabricated chip with 100-μm diameter holes (from Ref. 70, Figure 2). (*d*) SEM photograph of nerve tissue sections distal to a chip with hole diameters of 100 μm after 16 weeks of regeneration. Shown is a minifascicular pattern on the distal surface of the chip. The regenerated nerve structure has a smaller diameter than that of the perforated area of the chip. The circumferential perineural-like cell layer is clearly visible (from Ref. 70, Figure 5, *top*).

and other central neural elements into the cone took place. In 1998 at Emory University School of Medicine, two such electrodes were implanted into the brain of a paralyzed, speech-impaired patient. Such systems are able to control devices directly from the human central nervous system (78).

In 2000, cortical control using many more contacts [32 or 96 electrodes (wire arrays)] implanted into three motor areas of the monkey brain led to successful prediction of arm movements during a drinking task (79). The activity patterns recorded by the electrodes while the monkey performed the arm-movement trajectory could be translated into computer algorithms causing a robot arm to perform the same trajectory. Both of these developments show the feasibility of long-term brain-computer interfacing and control.

Other work (outside the scope of this paper because it involves no microelectrode interfacing) is the research on EEG-based brain-computer interfaces. The patient uses so-called motor imagery (they think about how they would perform a

movement, and the resulting EEG is real-time processed to control devices). The processing is mainly based upon event-related synchronization or desynchronization effects in the EEG patterns (80).

## PLANAR SUBSTRATE-EMBEDDED ELECTRODE ARRAYS

Planar Microelectrode Arrays for Cultured Neurons

Planar microelectrode arrays, consisting of transparent leads (indium tin oxide, or gold) to 10–100 electrode sites (diameter typically 10 μm) spaced at 100 μm interdistance on glass plates, were used by Thomas et al. (81), Gross (82, 83), Novak & Wheeler (84), and many others to study the activity and plasticity of developing cultured neuronal networks or brain slices. In this way, an attractive alternative was sought for the almost impossible job of probing many neurons simultaneously in a growing network with micropipettes. Two essential prerequisites for high-quality recordings are (*a*) lowering the high impedance of the tiny electrode sites to about 1 MΩ by additional electroplating of Pt-black (85) and (*b*) increasing the sealing resistance between cell and substrate by promoting adhesion. The latter can be achieved by coating the glass substrate with laminin, polylysine, or silane-based (mono)layers. Still, a number of neurons will adhere too far from the electrode sites to produce measurable action potentials. This finding led Tatic-Lucic et al. (86) to the discovery that the design of arrays consisting of electrode wells in which single embryonic neural somata were "locked up." In this design, only neurites should protrude from the wells to form neural networks. In this way, unique contacts are established, to be used as cultured bidirectional network probes. Alternatively, one can improve the contact efficiency by patterning the adhesive layer in detail; it is even possible to guide neural growth, for example, around and over electrodes. Both patterning and "cultured probes" are treated separately below.

Patterned Biological Neural Networks

Neuronal networks may be patterned in several ways. One method uses lasers to selectively cut cells away from a growing network (82). The other methods are chemical. One may modify neurophilic layers (like organosilanes, laminin, poly-D-lysine, polyethyleneimine) and neurophobic layers (like polyimid, glass, fluorocarbon) into the desired pattern by conventional lithographic and deposition methods (87–91). An illustration is presented in Figure 19. A faster way is the so-called microstamping method (92, 93) in which substrates are modified by printing the desired pattern onto them (Figure 20).

In principle, one might design neuronal network architectures as circuits to perform specific functions. The layout of chemical tracks would determine function. However, it is by no means certain that network growth is now sufficiently understood to yield reliable and functional connections at the extremely
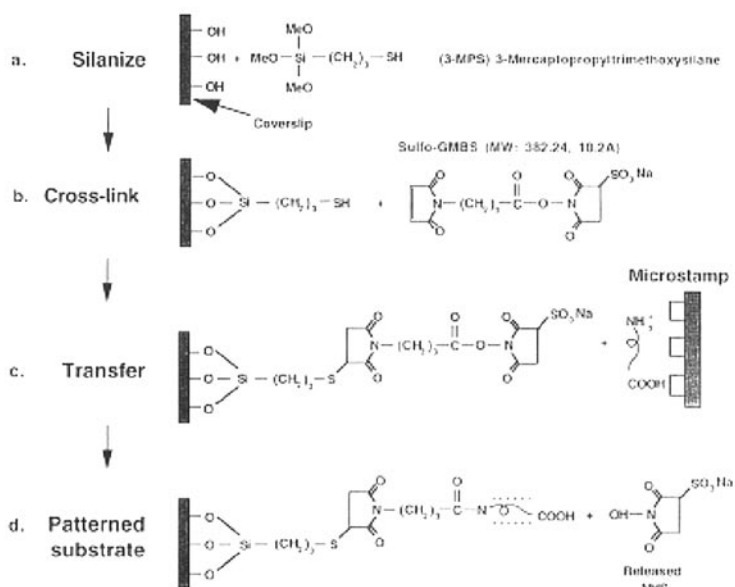
(a)

(b)
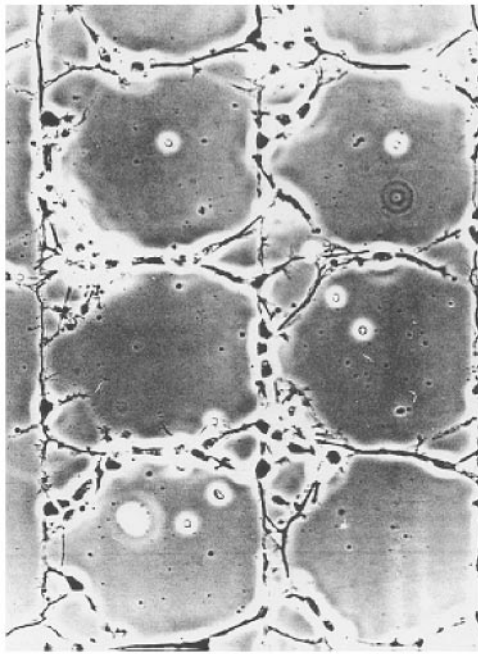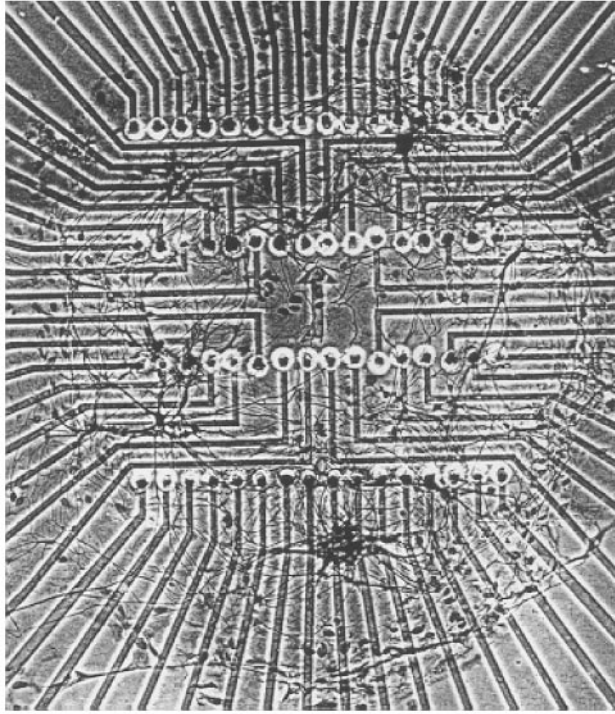
low local densities inherent in such networks. (See also the section below on creation by training methods of functional circuits in unpatterned networks.)

When the task of stimulation or recording concerns an axon or soma in vitro, the cell is lying over an electrode site in an MEA. This situation offers a controlled environment in which the cell adheres to known adhesion molecules, possibly after having been guided in a controlled way to an electrode location (Figure 21). Here the amount of electrode coverage and the quality of the sealing are in a controlled condition, reflected in the signal transfer between electrode and cell and in the electrode impedance (94–97). Although the in vitro situation is a controlled condition, cell functioning may still deviate from the normal situation. For example, membranes may adapt to the environment they are adhered to. The distribution of ionic channels in the membranes of the adhered parts of these cells may change and be reflected in an altered shape of the action potential (98, 99, 24). Ionic depletion in the narrow gap between adhered membrane and substrate may be responsible for altered intracellular and extracellular waveforms, in response to stimulation.
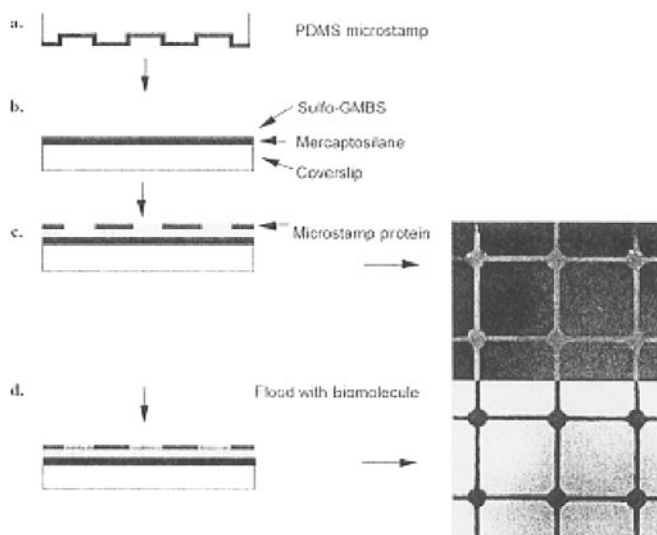
Cell-Cultured Multielectrode Probes

Cultured arrays may one day be used as cultured neuron probes, for example, by controlling each cell separately in a "cage" on a neurochip (100) or by controlling small networks at each electrode (101). They may be implanted in living nerve tissue to serve as a hybrid interface between electronics and nerve. The advantage would be that the electrode-cell interface may be established and optimized in the lab, while the nerve network after implantation may be a realistic target for ingrowth of nerve (collaterals). Figure 22 shows an eight-day-old hippocampal culture on a neurochip. Several neurites emerge from most of the wells. For survival of the neurons and delivering growth factors, a coverslip cultured with glia cells is put onto the neurochip with the glia facing the neuron surface 2 mm away. Figure 23a presents schematically the design of a cultured-probe neural prosthetic device. Each electrode has its own island of cultured cells adhered to the electrode's immediate environment. The cells provide an environment well adapted to collateral sprouts from the neural tissue where the probe is implanted.

Figure 19 (*a*) Low-density neuronal monolayer culture composed of 76 neurons growing over a matrix of 64 electrodes. The recording craters are spaced 40 μm laterally and 200 μm between rows. The transparent indium tin oxide conductors are 10 μm wide. Tissue is mouse spinal cord; culture age is 27 days in vitro; histology is Loots-modified Bodian stain (from Ref. 118, p. 284, Figure 2). (*b*) Cultured hippocampal neurons on patterned self-assembled monolayers. A hybrid substrate pattern of trimethyloxysilyl propyldiethylenetriamine (DETA) and perfluorated alkylsilane (13F) shows selective adhesion and excellent retention of the neurites to the DETA regions of the pattern (from Ref. 118, p.18, Figure 4).
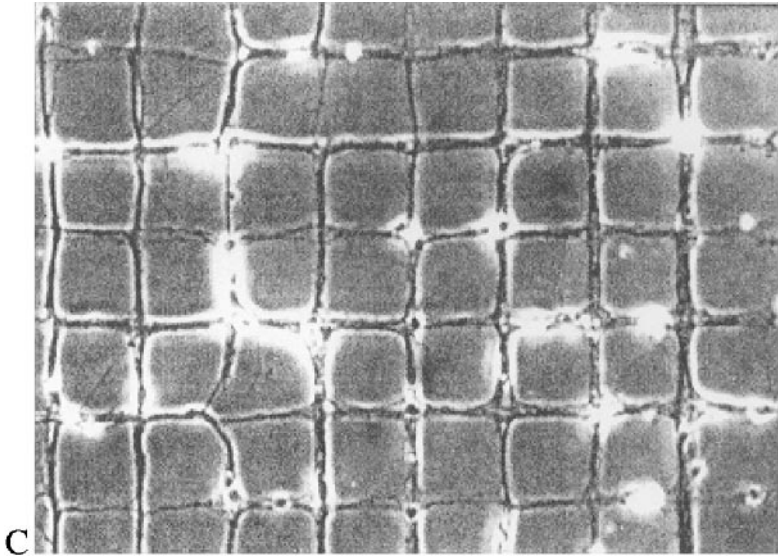
a. Silanize

b. Cross-link   Sulfo-GMBS (MW: 382.24, 10.2A)

c. Transfer

d. Patterned substrate

A

a. PDMS microstamp

b. Sulfo-GMBS / Mercaptosilane / Coverslip

c. Microstamp protein

d. Flood with biomolecule

B

Figure 20 (*A*) Microcontact printing, showing the silanization, cross-linking, and stamping process. The microstamp transfers polylysine from the places of contact to the glass coverslip. (*a*) Mercaptosilane linked to glass. (*b*) Sulfo-GMBS linked to mercaptosilane. (*c*) Polylysine transferred onto sulfo-GMBS and mercaptosilane-treated coverslip. (*d*) Final polylysine pattern linked to coverslip. (*B*) Microcontact printing, showing the microstamp procedure. (*a*) Absorbed polylysine on PDMS microstamp. (*b*) Silanized and cross-linked coverslip. (*c*) Microstamp transfers fluorescein isothiocyanate conjugated poly-l-lysine to coverslip, and (*d*) for this substrate, TRITC-labeled BSA was flooded and then imaged on a fluorescence microscope, showing the polylysine grid patterns. The microstamp pattern dimensions are 80 μm internodal length, 20 μm node diameter, and 5 μm line width. (*C*) Patterned hippocampal cells at 20 days in vitro, with polyethylene glycol (nonpermissive, or neurophobic, background, based on protein rejection). Dimensions as in Figure 20b, except 3 μm line width (from Ref. 93, Figures 1, 2, and 9a).

Figure 23b illustrates how cultured islands of neuronal cells can be patterned chemically on substrates.

STABILITY OF STIMULATION AND FUTURE APPLICATIONS

Chronic Implantation, Biocompatibility, and Stability of Interfaces

Chronic-implantation studies are important for the clinical application and acceptance of stimulation devices. For future use of microelectrode arrays in humans, biocompatibility and stability will become crucial.
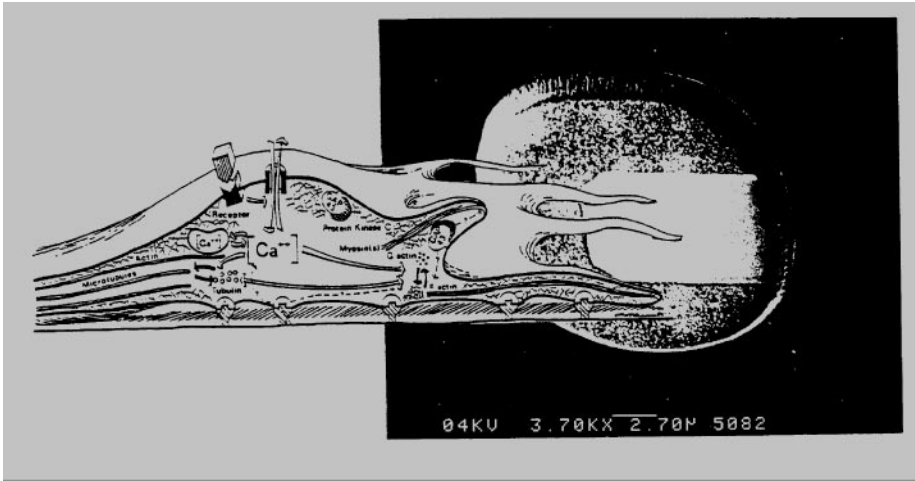
Figure 21   Impression of a growing nerve cell whose protruding axon is approaching a microelectrode site (well diameter is 12 μm). The growth cones (filopodia) find their way, guided by a complex machinery of secretion and reception of specific "semaphor" proteins, which may act over short and long distances. Protein-coated electrodes may take part in this machinery to seduce nerve cells.

Damage to neural tissue may consist of (reversible) swelling, connective tissue formation, and (irreversible) Wallerian degeneration. In general, the mechanisms responsible for damage may be of surgical, mechanical, or chemical origin. Cortical implantation of single- and multi-electrode wire devices seems in general to be performed today without problems. McCreery et al. (102) implanted single Ir microwire electrodes in cat cochlear nucleus and found tissue damage after long stimulation highly correlated to the amount of charge per phase. The safe threshold was 3 nC/phase (while stimulus threshold was about 1 nC/phase). Lefurge et al. (103) implanted Teflon-coated Pt-Ir wires, diameter 25 μm, intrafascicularly. They appeared to be tolerated well by cat nerve tissue for six months, causing little damage. Edell et al. (104) and Schmidt et al. (105) investigated the influence of silicon microshaft arrays on rabbit and cat cortical tissue. While neuron density around the 40 μm wide shafts decreased, adverse tissue response along the shafts was minimal over six months (104), except at the sharp tips. Rousche & Normann (106) reported on implantation of a densely packed needle-brush array (100 electrode sites) into feline cortex. They found no histological damage after three months of stimulation. (Stimulation occurred for 4 minutes a day; 11 electrodes were wired, and 7 were tracked for three months; average charges were 8.5, 8.6, and 11.6 nC/phase for three cats.)

Liu et al. (107) report that a seven-electrode array (iridium needles with lengths 1.5, 1.8, and 2 mm; 35 μm diameter; and 380 μm spacing) became stable after
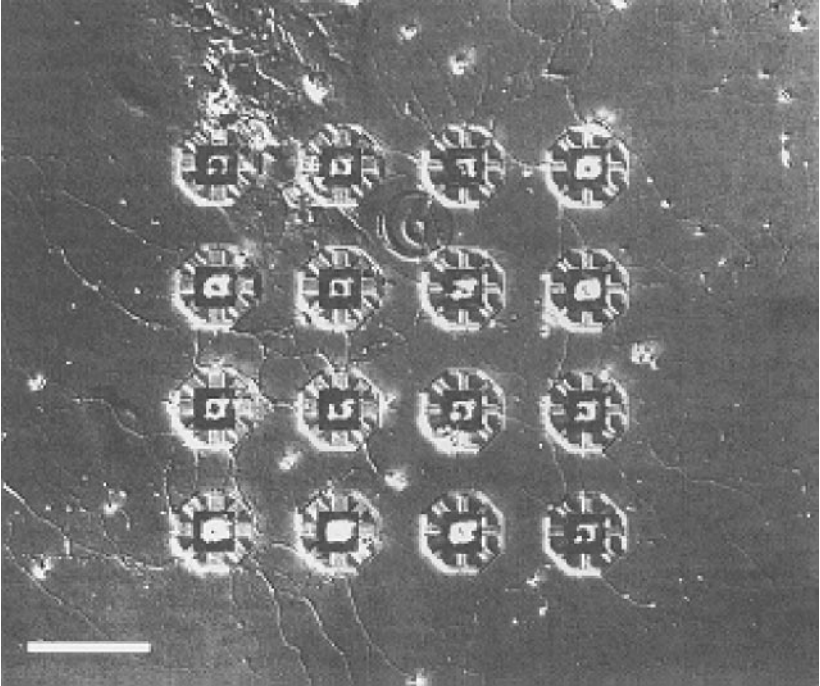
Figure 22 Micrograph of a hippocampal culture on a neurochip after 8 days in culture. Several neurites emerge from most wells. (Caged wells are covered by a silicon nitride canopy with a central hole; a freshly dissociated rat neuron is inserted into this hole; the neuron soma grows and locks itself in, and the neurites then emerge from the wells. To enable survival of the neurons and delivering growth factors, a coverslip cultured with glia cells is put onto the neurochip with the glia facing the neuron surface 2 mm away. The scale bar is 100 μm long (from Ref. 100, Figure 5).

two months of implantation in cat cortex. The lead to the device being mounted in a very flexible way through the dura and rigidly fixed to the skull, thereby allowing the device to operate in a "floating" way. In the first two months, although responsiveness of the electrodes changed, very little connective tissue formation around the electrodes was seen. Rutten et al. (108) found that, in peripheral nerve, six months after implantation of a one-dimensional silicon-based array (without leads) in rat peroneal nerve, a 10 μm thin connective tissue layer had grown around the array only. The gait of the implanted rats returned to normal within a few days of implantation. Both the minimal reaction to silicon oxide/silicon nitride and the normal gait suggest that such intraneural implants are tolerated well.

Of course, a large 3-D array, with a "nailbed" or brush shape, inserted into a nerve fascicle would occupy volume and would be expected to evoke a severe tissue reaction. Such an implantation has not yet been tried chronically. It would

be difficult to keep flexible the relatively bulky set of leads that would be involved with an array of, say, 100 electrodes; preferable would be the use of a local processing chip to reduce the number of wires to an acceptable number, in the range of 20.

Safe Stimulation

Safe stimulation aims at the prevention of damage to the neural tissue and to the electrode during long-term stimulation. The ideal is to stimulate only capacitively, but this limits the transferable charge seriously as the double-layer charge of a microelectrode is very small. Consequently, even at low current, one enters the Faradaic regime, reversibly or irreversibly. However, by avoiding irreversible chemical reactions and by choosing the right electrode materials, the aim of safety can be reached. Iridium oxide, for example, has a large reversible charge injection capacity, thus allowing high charge injection without Faradaic electrolysis (gassing limit is high) or net dc charge transfer. A number of charge-balanced stimulus waveforms, either sinusoidal or pulsatile (symmetric or asymmetric), are in use to date in neural stimulation to manage the electrode processes optimally.

Bursting Networks, Pharmacological Treatment, and Biosensor Applications

One of the most exciting new possibilities of modern MEA interfacing technology is the study of cellular and network functioning in vitro after pharmacological/biochemical treatment. Gross and coworkers especially are active in the use of cultured cells and networks as biosensors. Gross & Kowalski (109) concluded that all networks could be made active, be made more active, or be silenced chemically with great sensitivity to calcium, potassium, strychnine, bicuculline, glutamate, carbamazepine, and GABA, among many other substances (110). They also found that networks are never morphologically disconnected and are most generally characterized by oscillatory, entrained, or coarsely grained bursting phenomena in the neural discharge activity patterns. This was confirmed later by a number of other groups. We observed that spontaneous bursts (large-scale with many sites active) are typically separated on a time scale of minutes, while in-between a few "pacemakers" are active always. The whole pattern may change its characteristics (other pacemakers, other patterns of network bursts) on a scale of days, but the alternation of pacing and bursting stays (111).

Learning Networks

Another exciting new application is the biological "simulation" of developing brain-like networks. It is well known that our human brain is highly trainable owing to the plastic nature of its synaptic connections. It has been shown in the past two decades that artificial neural networks can likewise be trained to perform pattern recognition tasks by Hebbian synaptic-strength modification rules. These rules are based on what we know from single-cell or few-cell recordings in intact brain.

Might cultured neural networks comprising a relatively small numbers of elements (on the order of thousands of cells) teach us more about collective behavior, network functioning, and perhaps even about the function of the complete brain? Can neuronal networks be trained? A very recent positive answer came form Shahaf & Marom (4), who demonstrated that networks of cortical neurons can be trained in a remarkably simple and rapid way. They found that the network "explores a large space of possible connections and can be instructed to select and stabilize one or a subset of them by withdrawing the stimulus at the point that the connection is observed." The experiments were done by stimulating a specific electrode pair at a low rate (0.3, 0.5, or 1 Hz), with two distinct timing patterns (2 or 10 minutes on, 8 minutes off), until a predefined response was observed at 50 ms after the stimulus, at which time the stimulation was stopped and the procedure repeated. Ultimately the desired response is elicited directly. The authors conclude that the networks stabilize at response configurations that remove the stimuli, and they extend this conclusion speculatively to the behavioral concept of reward: The brain responds to stimuli in a nonexploratory way. This means that once a task has been learned, recognition characterizes itself by the absence of the exploration of possible solutions. (The principle here is very different from that of a reward model involving a separate mechanism.)

Other studies aim to train networks by feedback mechanisms in connection to real or computer-generated outer-world sensors [see, for example, DeMarse et al. (112)]. One criticism of overly optimistic extrapolation from cultured network properties to those of the brain is that, once they have been removed from neonatal animal brains, networks of dissociated cells have lost their native cell-neighbor relationships. Although this has not been studied conclusively yet, cultures with an organo-typic nature (brain slices) from rat brain have been shown morphologically and functionally to remain very natural and are therefore helpful tools (except during the first period of incubation) in developmental biology and pharmacology and as a substitute for experimental animals (113).

Neural Prostheses

It is hard to predict when neural prostheses, based on the foregoing devices and developments, will take their place in clinical practice, serving to restore lost or damaged functions or being used to enhance normal function. The process of developing laboratory prototypes (based on animal studies) into clinically applicable devices for humans is usually a long one and depends on many socioeconomical factors. To date, clinical human studies use mainly cuff microelectrodes (peripheral nerve), deep-brain (micro- and macro-) electrodes, and flexible (cochlear) array electrodes. Application of multielectrode systems is currently retarded by insufficient understanding of brain function and neural control.

In the lab, meanwhile, new approaches, such as the neurochip and the cultured probe mentioned above, are being sought. For a recent update on new developments, see the July 2001 Special Issue of the *Proceedings of the IEEE*, entitled "Neural engineering: merging engineering and neuroscience" (115).

FURTHER READING

A number of books can be recommended for further reading, for example, *Composition of Peripheral Nerves* by Boyd & Davey (116), *Neural Prostheses* by Agnew & McCreery (117), and *Enabling Technologies for Cultured Neural Networks* by Stenger & McKenna (118). For more details on neurophysiology (for example, on the Hodgkin-Huxley membrane model), see *Fundamental Neuroscience* by Zigmond et al. (119) or J.T. Mortimer's chapter in Agnew & McCreery's *Neural Prostheses* (117). For detailed overviews on microelectrode models, see Kovacs' chapter in Stenger & McKenna's *Enabling Technologies for Cultured Neural Networks* (118). Chapters 4 and 5 in *Neural Prostheses* (117) summarize in detail the mechanisms of neural damage caused by incorrect application of cuffs (mechanical stress), choice of the wrong electrode material, use of too-rigid leads, and several types of surgical trauma, among other problems.

The *Annual Review of Biomedical Engineering* is online at
http://bioeng.annualreviews.org

LITERATURE CITED

1. Galvani L. 1791. De viribus electricitatis in motu musculari, commentarius. *Bononiensi Sci. Artium Inst. Acad.* 7:363–418

2. Hodgkin AL, Huxley AF. 1952. A quantitative description of membrane current and its application to conduction and excitation in nerve. *J. Physiol.* 117:500–44

3. Brindley GS, Lewin WW. 1968. The sensations produced by electrical stimulation of the visual cortex. *J. Physiol.* 196:479–93

4. Shahaf G, Marom S. 2001. Learning in networks of cortical neurons. *J. Neurosci.* 21:8782–88

5. Grill WM, Kirsch RF. 1999. Neural prostheses. In *Wiley Encyclopedia of Electrical and Electronics Engineering*, ed. JG Webster, pp. 339–50. New York: Wiley

6. Veraart C, Raftopoulos C, Mortimer JT, Delbeke J, Pins D, et al. 1998. Visual sensations produced by optic nerve stimulation using an implanted self-sizing spiral cuff electrode. *Brain Res.* 813:181–86

7. Pfurtscheller G, Neuper C. 2001. Motor imagery and direct brain-computer interfaces. *Proc. IEEE* 89:1123–35

8. Mogilner AY, Benabid A-L, Rezai AR. 2001. Brain stimulation: current applications and future prospects. *Thalamus Relat. Syst.* I:255–67

9. Grinvald A. 1985. Real-time optical mapping of neuronal activity: from single growth cones to the intact brain. *Annu. Rev. Neurosci.* 8:263–305

10. Frankenhauser B, Huxley AF. 1964. The action potential in the myelinated nerve of Xenopus Laevis as computed on the basis of voltage clampodata. *J. Physiol.* 171:302–15

11. McNeal D. 1976. Analysis of a model for excitation of myelinated nerve. *IEEE Trans. Biomed. Eng.* 23:329–37

12. Rattay F. 1989. Analysis of models for extracellular fiber stimulation. *IEEE Trans. Biomed. Eng.* 36:676–83

13. Meier JH, Rutten WLC, Zoutman AE, Boom HBK, Bergveld P. 1992. Simulation of multipolar fiber selective neural stimulation using intrafascicular electrodes. *IEEE Trans. Biomed. Eng.* 39:122–34

14. Warman E, Grill WM, Durand D. 1992. Modeling the effect of electric fields

on nerve fibers: determination of excitation threshold. *IEEE Trans. Biomed. Eng.* 39:1244–54

15. Nagarajan S, Durand D. 1993. Effects of induced electric fields on finite neuronal structures: a simulation study. *IEEE Trans. Biomed. Eng.* 40:1175–88

16. Grill WM, Mortimer JT. 1996. The effect of stimulus pulse duration on selectivity of neural stimulation, *IEEE Trans. Biomed. Eng.* 43:161–66

17. Meier JH, Rutten WLC, Boom HBK. 1995. Force recruitment during electrical nerve stimulation with multipolar intrafascicular electrodes. *Med. Biol. Eng. Comput.* 33:409–17

18. Veltink PH, van Veen BK, Struijk JJ, Holsheimer J, Boom HBK. 1989. A modeling study of nerve fascicle stimulation. *IEEE Trans. Biomed. Eng.* 36:683–92

19. Goodall EV, Kosterman LM, Holsheimer J, Struijk JJ. 1995. Modeling study of size selective activation of peripheral nerve fibers with a tripolar cuff electrode. *IEEE Trans. Rehabil. Eng.* 3:272–82

20. Huang CQ, Sheperd RK, Carter PM, Seligman PM, Tabor B. 1999. Electrical stimulation of the auditory nerve: direct current measurement *in vivo. IEEE Trans. Biomed. Eng.* 46:461–71

21. Gielen FLH, Bergveld P. 1982. Comparison of electrode impedances of Pt, PtIr (19% Ir) and Ir-AIROF elctrodes used in electrophysiological experiments. *Med. Biol. Eng. Comput.* 20:77–83

22. de Boer RW, van Oosterom A. 1978. Electrical properties of platinum electrodes: impedance measurements and time-domain analysis. *Med. Biol. Eng. Comput.* 16:1–10

23. Ranck JB. 1975. Which elements are excited in electrical stimulation of the mammalian central nervous system: a review. *Brain Res.* 98:417–40

24. Buitenweg JR. 2001. *Extracellular stimulation window explained by a geometry based model of the neuron-electrode contact.* PhD thesis. University Twente, Netherlands, Chapter 6. Enschede: Twente Univ. Press. 123 pp.

25. Smit JPA. 1996. *Selective motor stimulation using endoneural prosthesis.* PhD thesis. University of Twente, Netherlands. Enschede: Twente Univ. press. 105 pp.

26. Rutten WLC, van Wier H, Put JMH. 1991. Sensitivity and selectivity of intraneural stimulation using a silicon electrode array. *IEEE Trans. Biomed. Eng.* 38:192–98

27. Rutten WLC, Smit JPA, Bielen JA. 1997. Two-dimensional neuro-electronic interface devices: force recruitment, selectivity and efficiency. *Cell. Eng.* 2:132–37

28. Smit JPA, Rutten WLC, Boom HBK. 1999. Endoneural selective stimulation using wire-microelectrode arrays. *IEEE Trans. Rehabil. Eng.* 7:399–412

29. Rijkhoff NJM, Holsheimer J, Koldewijn EL, Struijk JJ, van Kerrebroeck PEV, et al. 1994. Selective stimulation of sacral nerve roots for bladder control: a study by computer modeling. *IEEE Trans. Biomed. Eng.* 41:413–25

30. Rutten WLC, Smit JPA, Rozijn TH, Meier JH. 1995. 3D Neuro-electronic interface devices for neuromuscular control: design studies and realisation steps. *Biosens. Bioelectron.* 10:141–53

31. Pickard RS. 1979. A review of printed circuit microelectrodes and their production. *J. Neurosci. Methods* 1:301–18

32. Drake KL, Wise KD, Farraye J, Anderson DJ, BeMent SL. 1988. Performance of planar multisite microprobes in recording extracellular single-unit intracortical activity. *IEEE Trans. Biomed. Eng.* 35:719–32

33. Evans JK, Niparko JM, Miller JM, Jyung R, Anderson DJ. 1989. Multiple-channel stimulation of the cochlear nucleus. *Otolaryngol. Head Neck Surg.* 101:651–57

34. Anderson DJ, Najafi K, Tanghe SJ, Evans DA, Levy KL, et al. 1989. Batch-fabricated thin-film electrodes for stimulation of the central auditory system. *IEEE Trans. Biomed. Eng.* 36:693–704

35. Tanghe SJ, Najafi K, Wise KD. 1990. A Planar IrO multichannel stimulating electrode for use in neural prostheses. *Sens. Actuators B* 1:464–67

36. Ji J, Najafi K, Wise KD. 1990. A scaled electronically-configurable multichannel recording array. *Sens. Actuators A* 22:589–91

37. Ji J, Wise KD. 1992. An implantable CMOS circuit interface for multiplexed microelectrode recording arrays. *IEEE J. Solid-State Circuits* 26:433–43

38. Tanghe SJ, Wise KD. 1992. A 16-channel CMOS neural stimulating array. *IEEE J. Solid-State Circuits* 27:1819–25

39. Hoogerwerf AC, Wise KD. 1994. A 3D micro-electrode array for chronic neural recording. *IEEE Trans. Biomed. Eng.* 41:1136–46

40. Kim C, Wise KD. 1996. A 64-site multishank CMOS low-profile neural stimulating probe. *IEEE J. Solid-State Circuits* 31:1230–38

41. Kewley DT, Hills MD, Borkholder DA, Opris IE, Maluf NI, et al. 1997. Plasma-etched neural probes. *Sens. Actuators A* 58:27–35

42. Najafi K, Ji J, Wise KD. 1990. Scaling limitations of silicon multichannel recording probes. *IEEE Trans. Biomed. Eng.* 37:1–11

43. Najafi K, Hetke JF. 1990. Strength characterization of silicon microprobes in neurophysiological tissues. *IEEE Trans. Biomed. Eng.* 37:474–81

44. Hetke JF, Najafi K, Wise KD. 1990. Flexible miniature ribbon cables for long-term connection to implantable sensors. *Sens. Actuators A* 23:999–1002

45. Hetke JF, Lund JL, Najafi K, Wise KD, Anderson DJ. 1994. Silicon ribbon cables for chronically implantable microelectrodes arrays. *IEEE Trans. Biomed. Eng.* 41:314–21

46. Akin T, Ziaie B, Nikles SA, Najafi K. 1999. A modular micromachined high-density connector system for biomedical applications. *IEEE Trans. Biomed. Eng.* 46:471–81

47. Suaning GJ, Lovell NH. 2001. CMOS neurostimulation ASIC with 100 channels, scaleable output and bidirectional radio-frequency telemetry. *IEEE Trans. Biomed. Eng.* 48:248–61

48. Rutten WLC, Droog A, Rouw M, Smit JPA. 1999. A gate-array/multi-electrode device: circuit performance and interfacing. *Proc. Joint BMES/IEEE-EMBS Conf.*, 1st, Atlanta, 1999

49. Campbell PK, Jones KE, Huber RJ, Horch K, Normann RA. 1991. A silicon-based three-dimensional neural interface: manufacturing processes for an intracortical electrode array. *IEEE Trans. Biomed. Eng.* 38:758–68

50. Nordhausen CT, Rousche PJ, Normann RA. 1994. Optimizing recording capabilities of the Utah intracortical electrode array. *Brain Res.* 637:27–36

51. Frieswijk TA, Rutten WLC, Kerkhoff HG, Lippe K. 1995. Control electronics for a neuro-electronic interface implemented in a gate array. *Proc. Int. Conf. IEEE Biomed. Eng. Soc.*, 17th, Montreal, 1995

52. Frieswijk TA, Bielen JA, Rutten WLC, Bergveld P. 1997. Development of a solder bump technique for contacting a three-dimensional multi electrode array. *Microsyst. Technol.* 1:48–52

53. Ehrfeld W, Munchmeyer D. 1991. LIGA method, three dimensional microfabrication using synchrotron radiation. *Nucl. Instr. Methods Phys. Res. A* 303:523–31

54. Rutten WLC, Smit JPA, Bielen JA. 1997. Two-dimensional neuro-electronic interface devices: force recruitment, selectivity and efficiency. *Cell. Eng.* 2:132–37

55. Malagodi M, Horch KW, Schoenberg AA. 1989. An intrafascicular electrode for recording of action potentials in peripheral nerves. *Ann. Biomed. Eng.* 17:397–410

56. Nannini N, Horch K. 1991. Muscle recruitment with intrafascicular electrodes. *IEEE Trans. Biomed. Eng.* 38:769–76

57. Goodall EV, Horch KW. 1992. Separation of action potentials in multi-unit intrafascicular recordings. *IEEE Trans. Biomed. Eng.* 39:289–95

58. McNaughton T, Horch K. 1994. Action potential classification with dual channel intrafascicular electrodes. *IEEE Trans. Biomed. Eng.* 41:609–16

59. McNaughton TG, Horch KW. 1996. Metallized polymer fibers as leadwires and intrafascicular microelectrodes. *J. Neurosci. Methods* 70:103–10

60. Yoshida K, Horch K. 1993. Reduced fatigue in electrically stimulated muscle using dual channel intrafascicular electrodes with interleaved stimulation. *Ann. Biomed. Eng.* 21:709–14

61. Yoshida K, Horch K. 1996. Closed-loop control of ankle position using muscle afferent feedback with functional neuromuscular stimulation. *IEEE Trans. Biomed. Eng.* 43:167–76

62. Hoffer JA, Marks WB, Rymer WZ. 1974. Nerve fiber activity during normal movements. *Soc. Neurosci. Abstr.* 4:300

63. Stein RB, Charles D, Davis L, Jhamandas J, Mannard A, et al. 1975. Principles underlying new methods for chronic neural recording. *Can. J. Neurol. Sci.* 2:235–44

64. van den Honert C, Mortimer JT. 1981. A technique for collision block of peripheral nerve. *IEEE Trans. Biomed. Eng.* 28:373–82

65. Fang ZP, Mortimer JT. 1987. A method for attaining natural recruitment order in artificially activated muscles. *Proc. 9th Int. Annu. Conf. IEEE Biomed. Eng. Soc.*, Boston, 1987, pp. 657–58

66. Meier JH, Rutten WLC, Boom HBK. 1998. Extracellular potentials from active myelinated fibers inside a peripheral nerve. *IEEE Trans. Biomed. Eng.* 45:1146–54

67. Edell DJ. 1986. A peripheral nerve information transducer for amputees: long-term multichannel recordings from rabbit peripheral nerves. *IEEE Trans. Biomed. Eng.* 33:203–14

68. Kovacs GTA, Storment CW, Rosen JM. 1992. Regeneration microelectrode array for peripheral nerve recording and stimulation. *IEEE Trans. Biomed. Eng.* 39:893–902

69. Kovacs GTA, Storment CW, Halks-Miller M, Belczynski CR, Della Santina CC, et al. 1994. Silicon-substrate micro-electrode arrays for parallel recording of neural activity in peripheral and cranial nerves. *IEEE Trans. Biomed. Eng.* 41:567–77

70. Zhao Q, Drott J, Laurell T, Wallman L, Lindström K, et al. 1997. Rat sciatic nerve regeneration through a micromachined silicon chip. *J. Biomater.* 18:75–80

71. Blau A, Ziegler Ch, Heyer M, Schwitzgebel G, Matthies T, et al. 1997. Characterization and optimization of microelectrode arrays for in-vivo nerve signal recording and stimulation. *Biosens. Bioelectron.* 12:883–92

72. Wallman L, Levinsson A, Schouenborg J, Holberg H, Montelius L, et al. 1999. Perforated silicon nerve chips with doped registration electrodes, in vitro performance and in vivo operation. *IEEE Trans. Biomed. Eng.* 46(9):1065–74

73. Navarro X, Calvet S, Rodriguez FJ, Stieglitz T, Blau C, et al. 1998. Stimulation and recording from regenerated peripheral nerve through polyimide sieve electrodes. *J. Peripher. Nerv. Syst.* 3(2):91–101

74. Heiduschka P, Romann I, Stieglitz T, Thanos S. 2001. Perforated microelectrode arrays implanted in the regenerating adult central nervous system. *Exp. Neurol.* 171(1):1–10

75. Schlosshauer B, Brinker T, Maller HW, Meyer JU. 2001. Towards microelectrode implants: in vitro guidance of rat spinal cord neurites through polyimide sieves by Schwann cells. *Brain Res.* 903(1–2):237–41

76. Kennedy PR. 1989. The cone electrode: a long-term electrode that records from neurites grown onto its recording surface. *J. Neurosci. Methods* 29:181–93

77. Kennedy PR, Mirra SS, Bakay RA. 1992. The cone electrode; ultrastructural studies following long-term recording in rat and monkey cortex. *Neurosci. Lett.* 142(1):89–94

78. Kennedy PR, Bakay RA, Moore MM, Adams K, Goldwaithe J. 2000. Direct control of a computer from the human nervous system. *IEEE. Trans. Rehab. Eng.* 8(2):198–202

79. Wessberg J, Stambaugh C, Kralik J, Beck P, Laubach M, et al. Real-time prediction of hand trajectory by ensembles of cortical neurons in primates. *Nature* 408:361–65

80. Guger C, Ramoser H, Pfurtscheller G. 2000. Real time EEG analysis with subject-specific spatial patterns for a brain-computer interface (BCI). *IEEE Trans. Rehab. Eng.* 8(4):447–57

81. Thomas CA, Springer PA, Loeb GE, Berwald-Netter Y, Okun LM. 1972. A miniature microelectrode array to monitor the bioelectric activity of cultured cells. *Exp. Cell Res.* 74:61–66

82. Gross GW. 1979. Simultaneous single unit recording in vitro with a photoetched laser deinsulated gold multimicroelectrode surface. *IEEE Trans. Biomed. Eng.* 26:273–79

83. Gross GW, Wen WY, Lin JW. 1985. Transparant indium-tin oxide electrode patterns for extracellular, multisite recording in neuronal cultures. *J. Neurosci. Methods* 15:243–52

84. Novak JL, Wheeler BC. 1986. Recording from the Aplysia abdominal ganglion with a planar microelectrode array. *IEEE Trans. Biomed. Eng.* 33:196–202

85. Nisch W, Bock J, Egert U, Hammerle H, Mohr A. 1994. A thin film microelectrode array for monitoring extracellular neuronal activity in vitro. *Biosens. Bioelectron.* 9:737–41

86. Tatic-Lucic S, Tai Y-C, Wright JA, Pine J. 1993. Silicon-micromachined neurochips for in-vitro studies of cultured neural networks. *Proc. 7th Int. Conf. Solid State Sens. Acuators.*, pp. 943–46

87. Kleinfeld D, Kahler K, Hockberger P. 1988. Controlled outgrowth of dissociated neurons on patterned substrates. *J. Neurosci.* 8:4098–120

88. Ranieri JP, Bellamkonda R, Bekos EJ, Gardella A, Mathieu HJ, et al. 1994. Spatial control of neuronal cell attachment and differentiation on covalently patterned laminin oligopeptide substrates. *Int. J. Dev. Neurosci.* 12(8):725–35

89. Clemence JF, Ranieri JP, Aebischer P, Sigrist H. 1995. Photoimmobilization of a bioactive laminin fragment and pattern-guided selective neuronal cell attachment. *Bioconjug. Chem.* 6(4):411–17

90. Corey JM, Wheeler BC, Brewer GJ. 1996. Micrometer resolution silane-based patterning of hippocampal neurons: a comparison of photoresist and laser ablation methods of fabricating substrates. *IEEE Trans. Biomed. Eng.* 43:944–55

91. Ruardij TG, Goedbloed MH, Rutten WLC. 2000. Adhesion and patterning of cortical neurons on polyethyleneimine- and fluorocarbon coated surfaces. *IEEE Trans. Biomed. Eng.* 47:1593–600

92. Branch DW, Corey JM, Weyhenmeyer JA, Brewer GJ, Wheeler BC. 1998. Microstamp patterns of biomolecules for high-resolution neuronal networks. *Med. Biol. Eng. Comput.* 36:135–41

93. Branch DW, Wheeler BC, Brewer GJ, Leckband DA. 2000. Long-term maintenance of patterns of hippocampal pyramidal cells on substrates of polyethylene glycol and microstamped polylysine. *IEEE Trans. Biomed. Eng.* 47:290–301

94. Weis R, Fromherz P. 1997. Frequency dependent signal transfer in neuron transistors. *Phys. Rev. E* 55:877–89

95. Bove M, Grattarola M, Verreschi G. 1997. In vitro 2-D networks of neurons characterized by processing the signals recorded with a planar microtransducer array. *IEEE Trans. Biomed. Eng.* 44(10):964–78

96. Stett B, Muller P, Fromherz P. 1997. Two-way silicon-neuron interface by electrical induction. *Phys. Rev. E* 55:1779–82

97. Buitenweg JR, Rutten WLC, Willems WPA, van Nieuwkasteele JW. 1998. Measurement of sealing resistance of cell-electrode interfaces in neuronal cultures using impedance spectroscopy. *Med. Biol. Eng. Comput.* 36:630–37

98. Fromherz P. 1999. Extracellular recording with transistors and the distribution of ionic conductances in a cell membrane. *Eur. Biophys. J.* 28:254–58

99. Vassanelli S, Fromherz P. 1999. Transistor probes local potassium conductances in the adhesion region of cultured rat hippocampal neurons. *J. Neurosci.* 19:6767–73

100. Maher MP, Pine J, Wright J, Tai Y-C. 1999. The neurochip: a new multielectrode device for stimulating and recording from cultured neurons. *J. Neurosci. Methods* 87:45–56

101. Rutten WLC, Mouveroux JM, Buitenweg J, Heida T, Ruardij, et al. 2001. Neuroelectronic interfacing with cultured multi electrode arrays toward a cultured probe. *Proc. IEEE* 89:1013–29

102. McCreery DB, Yuen TGH, Agnew WF, Bullara LA. 1994. Stimulus parameters affecting issue injury during microstimulation in the cochlear nucleus of the cat. *Hear. Res.* 77:105–15

103. Lefurge T, Goodall E, Horch K, Stensaas L, Schoenberg A. 1991. Chronically implanted intrafascicular recording electrodes. *Ann. Biomed. Eng.* 19:197–207

104. Edell DJ, Toi VV, McNeil VM, Clark LD. 1992. Factors influencing the biocompatibility of insertable silicon microshafts in cerebral cortex. *IEEE Trans. Biomed. Eng.* 39:635–43

105. Schmidt S, Horch K, Normann R. 1993. Biocompatibility of silicon-based electrode arrays implanted in feline cortical tissue. *J. Biomed. Mat. Res.* 27:1393–99

106. Rousche PJ, Normann RA. 1999. Chronic intracortical microstimulation (ICMS) of cat sensory cortex using the Utah intracortical electrode array. *IEEE Trans. Rehab. Eng.* 7:56–69

107. Liu X, McCreery DB, Carter RR, Bullara LA, Yuen TGH, Agnew WF. 1999. Stability of the interface between neural tissue and chronically implanted microelectrodes. *IEEE Trans. Rehab. Eng.* 7:315–26

108. Rutten WLC, van Wier H, Put JMH, Rutgers R, de Vos RAI. 1988. Sensitivity, selectivity and bioacceptance of an intraneural multielectrode stimulation device in silicon technology. In *Electrophysiological Kinesiology*, ed. W Wallinga, HBK Boom, J de Vries, pp. 135–39. Amsterdam: Excerpta Medica

109. Gross GW, Kowalski JM. 1991. Experimental and theoretical analysis of random nerve cell network dynamics. In *Neural Networks: Concepts, Applications and Implementations*, ed. P Antognetti, V Milutinovic, 4:47–110. Prentice-Hall

110. Gross GW, Harsch A, Rhoades BK, Gopel W. 1997. Odor, drug and toxin analysis with neuronal networks in vitro: extracellular array recordings of network responses. *Biosens. Bioelectron.* 12:373–93

111. Rutten WLC, Ruardij TG, van Pelt J. 2001. Neuronal networks on 'cultured probe' micro electrode arrays: network confinement and activity patterns. *Proc. Atl. Symp. Comp. Biol. Genome Inform. Syst. Technol.*, pp. 101–105. Assoc. Intell. Mach

112. DeMarse TB, Wagenaar DA, Blau AW, Potter SM. 2001. The neurally controlled Animat: biological brains acting with simulated bodies. *Autonomous Robots* 11:305–11

113. Fennrich S, Stier H, Fohr K-J, Ray D, Ghersi-Egea JF, et al. 1996. Organotypic rat brain culture as in vivo–like model system. *Methods Cell Sci.* 18:283–91

114. Branner A, Stein RB, Normann RA. 2001. Selective stimulation of cat sciatic nerve using an array of varying-length microelectrodes. *J. Neurophysiol.* 85:1585–94

115. Akay M, ed. 2001. *Neural Engineering: Merging Engineering & Neuroscience.* Spec. Issue Proc. IEEE 89(7):991–1139

116. Boyd IA, Davey MR. 1968. *Composition of Peripheral Nerves*. Edinburgh: ES Livingstone. 57 pp.

117. Agnew WF, McCreery DB, eds. 1990. *Neural Prostheses Fundamental Studies*. Englewood Cliffs: Prentice-Hall. 322 pp.

118. Stenger DA, McKenna TM, eds. 1994. *Enabling Technologies for Cultured Neu-ral Networks*. San Diego: Academic. 355 pp.

119. Zigmond MJ, Bloom FE, Landis SC, Roberts JL, Squire LR, eds. 1999. *Fundamental Neuroscience*. San Diego: Academic. 1600 pp.

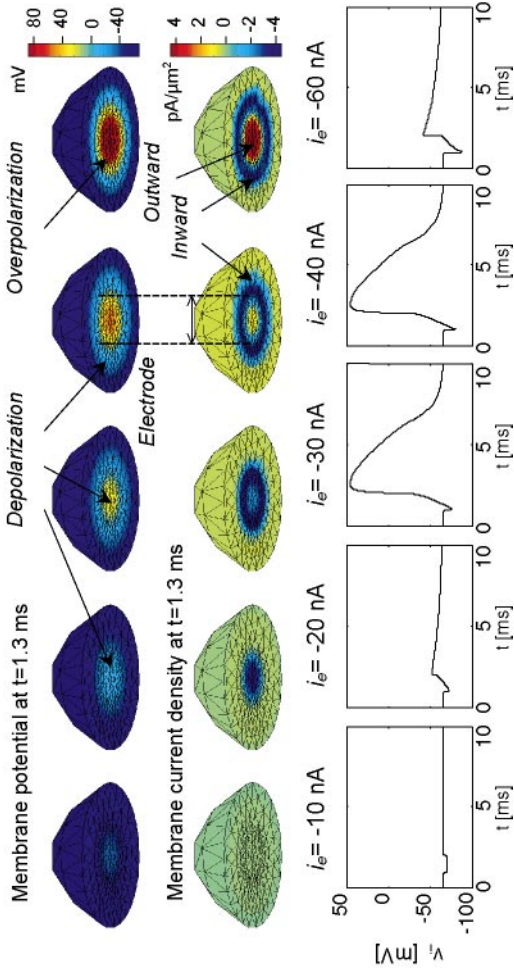120. Reilly JP. 1992. *Electrical Stimulation and Electropathology*. Cambridge: Cambridge Univ. Press. 504 pp.

Figure 8 Extracellular stimulation with several stimulus amplitudes. The intracellular responses to rectangular current pulses starting at t = 1 ms are plotted in the lower diagrams for stimulus amplitudes of −10, −20, −30, −40 and −60 nA. For each stimulus amplitude, the distribution of local membrane potentials (*top row*) and the local membrane current densities (*second row*) are depicted at t = 1.3 ms. (from Ref. 24, courtesy J. Buitenweg).
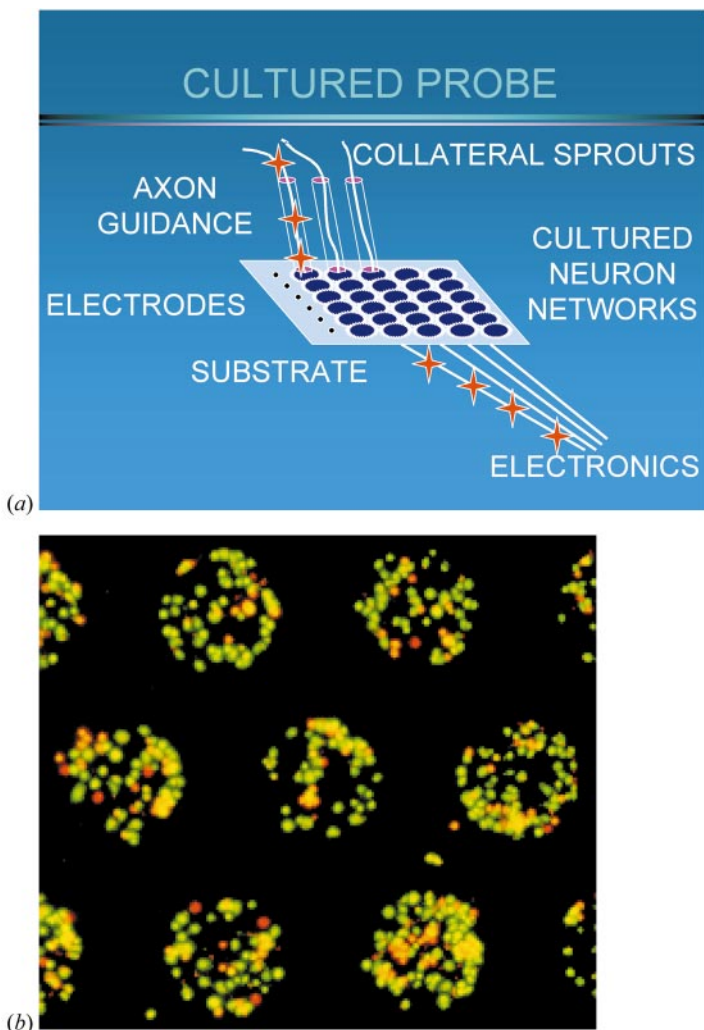
Figure 23 (*a*) Schematic impression of a cultured probe neural prosthetic device. Electrodes are patterned on an implantable (glass) substrate, each covered by a local network of cultured neurons before implantation. The networks are separated from each other by adhesive treatment of the substrate. They serve as natural hosts for collateral sprouts guided from the natural tissue towards the implanted interface device. A highly efficient neuroelectronic device results. Important research aspects are cell-electrode adhesion, trapping of cells, adhesion of local neural networks, and sprouting of collateral fibers (from Ref. 101, Figure 3). (*b*) Fluorescent image of acridine orange (*green*)-propidium iodide (*red*) stained cortical neurons (live or dead, respectively) on polyethylene imine-coated "islands" with a diameter of $150\,\mu$m. Results are shown after 1 day in vitro. Dark areas outside the circles represent the nonpermissive (neurophobic) fluorocarbon-coated layer (from Ref. 101, Figure 17a).